Electrochemical Kinetics of Corrosion and Passivity

The basis of a rate expression for an electrochemical process is Faraday's law:

$$m = \frac{Ita}{nF}$$

Where m is the mass reacted, I is the measured current in ampere, t is the time, a is the atomic weight, n the number of electrons transferred and F is the Faraday constant (96500 $Cmol^{-1}$). Dividing Faraday's law by the surface area A and the time t leads to an expression for the corrosion rate r:

$$r = \frac{m}{tA} = \frac{ia}{nF}$$

With the current density i defined as i = I/A.

Exchange current density:

We consider the reaction for the oxidation/reduction of hydrogen:

$$2H^+ + 2e^- \underset{r_r}{\overset{r_f}{\rightleftharpoons}} H_2$$

This reaction is in the equilibrium state at the standard half cell potential $e^0(H^+/H_2)$. This means that the forward reaction rate r_f and the reverse reaction rate r_r have the same magnitude. This can be written as:

$$r_f = r_r = \frac{i_0 a}{nF}$$

In this case is i_0 the exchange current density equivalent to the reversible rate at equilibrium. In other words, while the standard half cell potential e^0 is the universal thermodynamic parameter, i_0 is the fundamental kinetic parameter of an electrochemical reaction. The exchange current density cannot be calculated. It has to be measured for each system. The following figure shows that the exchange current density for the hydrogen reaction depends strongly on the electrode material, whereas the standard half cell potential remains the same.

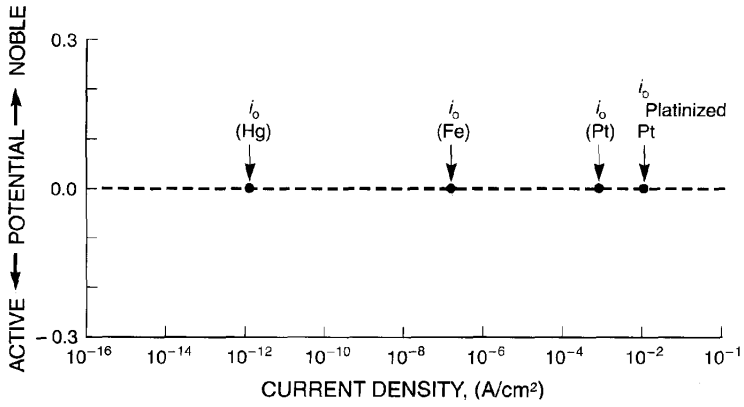

Electrochemical Polarization:

Polarization η is the change in the standard half cell potential e caused by a net surface reaction rate. Cathodic polarization η_c means that electrons are supplied to the surface and they build up a negative potential in the metal. Therefore η_c is negative by definition. Anodic polarization η_a is the opposite process. There are two different kinds of polarization (sometimes also known as overpotential) namely activation and concentration polarization.

Activation Polarization:

In this case a step in the half cell reaction controls the rate of electron (charge) flow. For example the hydrogen evolution reaction

$$2H^+ + 2e^- \rightarrow H_2$$

proceeds at a metal surface in three major steps. In the first step H+ reacts with an electron from the metal to form an adsorbed hydrogen atom at the surface.

$$H^+ + e^- \rightarrow H_{ads}$$

In the second steps the reaction of two adsorbed hydrogen atoms forms a hydrogen molecule.

$$H_{ads} + H_{ads} \rightarrow H_{2ads}$$

In the third step enough adsorbed hydrogen molecules combine and nucleate a hydrogen bubble on the surface. Any of these steps can be the rate limiting step and therefore cause the activation polarization. The activation polarization can be calculated using the current densities, which represent the reaction rates. For cathodic η_c and anodic η_a polarization one can write:

$$\eta_c = \beta_c \log \frac{i_c}{i_0}$$

$$\eta_a = \beta_a \log \frac{i_a}{i_0}$$

For zero η both equations reduce to i = i_0. For polarization potentials below the equilibrium half cell potential the reduction or forward reaction is favored:

$$2H^+ + 2e^- \rightarrow H_2$$

while above the half cell potential the reverse reaction is favored.

$$H_2 \rightarrow 2H^+ + 2e^-$$

In the figure the so called Tafel plot is shown. It depicts the change in the polarization potential with the current density.

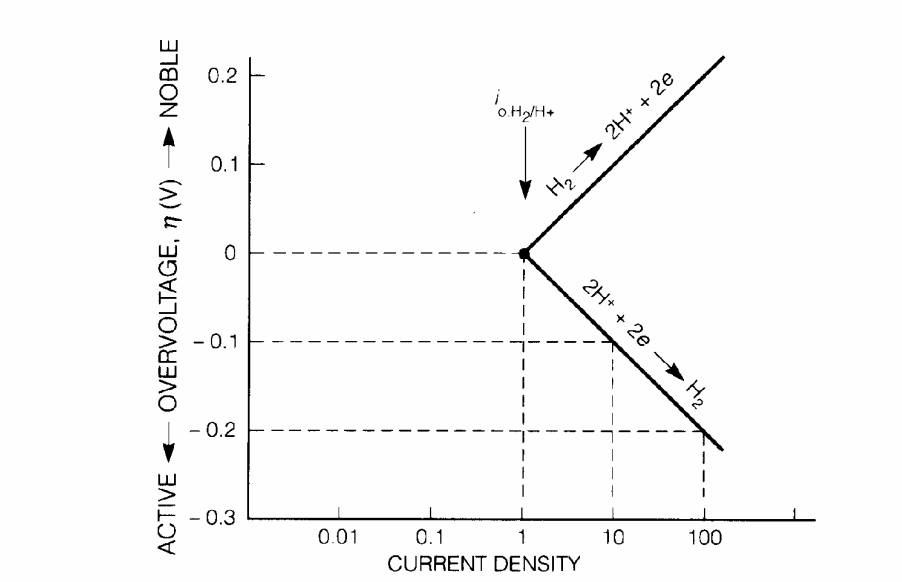

The activation polarization is related to the activation energy of the rate limiting step. Therefore a thermodynamical derivation of β is possible.

Concentration Polarization:

If the reaction on the metal surface is fast it can lead to a depletion of the adjacent solution of the dissolved species that reacts on the surface. This is shown for the H^+ concentration in the next figure. c_B is the H+ concentration in the bulk of the solution.

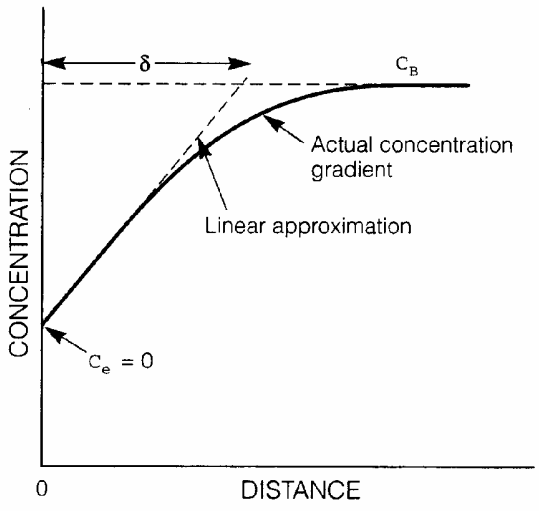

From the Nernst equation it is clear that the half cell potential is dependent on the H^+ concentration, in the form that the potential decreases with decreasing concentration.

$$e_{H^+/H_2} = e^0_{H^+/H_2} + \frac{2.3RT}{nF}\log\frac{\left(H^+\right)^2}{p_{H_2}}$$

The decrease in the half cell potential is the concentration polarization η_{conc}, which can be written in terms of current density using the Nernst equation as:

$$\eta_{conc} = \frac{2.3RT}{nF}\log\left[1 - \frac{i_c}{i_L}\right]$$

A plot of this equation can be seen in the next figure. One can see that η_{conc} is low until a limiting current density i_L is reached. This current density is the measure of a maximum reaction rate that cannot be exceeded because of a limited diffusion rate of H^+ within the solution. The limiting current density can be calculated as follows:

$$i_L = \frac{D_Z nFC_B}{\delta}$$

D_Z is the diffusivity of the reacting species Z, C_B is the concentration in the bulk of the solution and δ is the thickness of the depleted zone. i_L is increased with increasing concentration, with increasing diffusivity (temperature) and higher solution agitation, which

decreases δ.

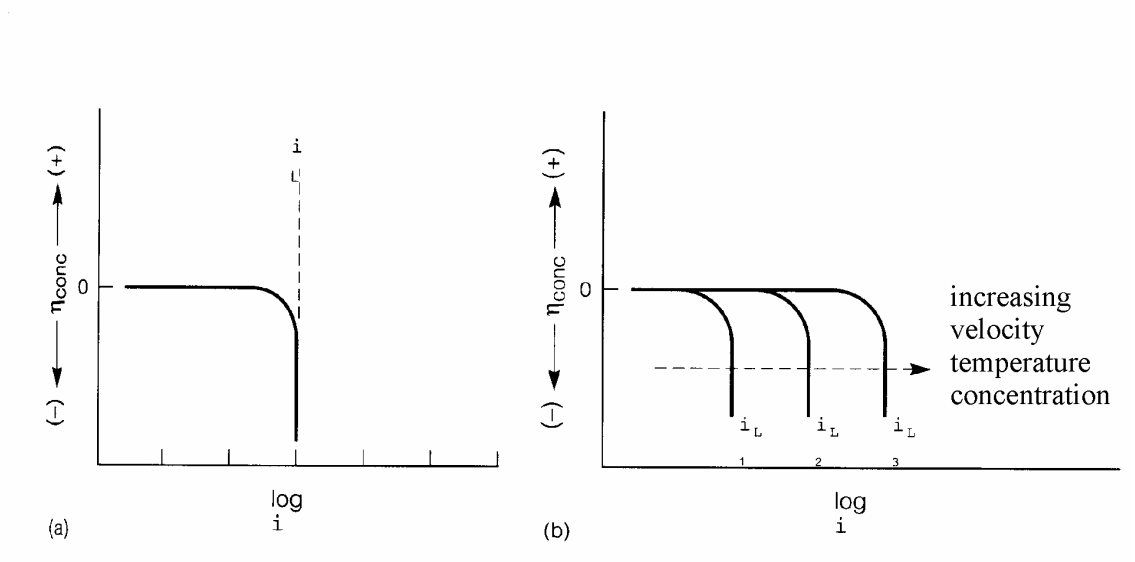

Concentration polarization is only significant for cathodic reduction processes, as for anodic oxidation one usually has an unlimited supply of metal atoms at the interface. Only at very high corrosion rates or during intentional anodic dissolution by an impressed current one can find concentration polarization due to limited rates of transport of soluble oxidation products away from the surface.

Mixed Potential Theory:

Charge conservation is required to apply the equations derived for polarization potentials. This means that the sum of anodic oxidation currents must equal the sum of cathodic reduction currents. For anodic oxidation there is one reaction of the general form:

$$M \rightarrow M^{n+} + ne^-$$

There are basically three different kinds of cathodic reactions:

1. Evolution of Hydrogen from acid or neutral solutions:

$$2H^+ + 2e^- \rightarrow H_2 \quad \text{(acid solutions)}$$

$$2H_2O + 2e^- \rightarrow H_2 + 2OH^- \quad \text{(neutral and alkaline solutions)}$$

2. Reduction of dissolved oxygen in acid or neutral solutions:

$$O_2 + 4H^+ + 4e^- \rightarrow 2H_2O \quad \text{(acid solutions)}$$

$$O_2 + 2H_2O + 4e^- \rightarrow 4OH^- \quad \text{(neutral and alkaline solutions)}$$

3. Reduction of a dissolved oxidizer in a redox reaction (e.g.):

$$Fe^{3+} + e^{-} \rightarrow Fe^{2+}$$

Corrosion Potential E_{corr}:

When two half cell reactions occur simultaneously on a metal surface, both of them will change the potential to an intermediate value called the corrosion potential. At the corrosion potential all the rates (current densities) are equal: $i_c = i_a = i_{corr}$. This is schematically shown in the figure.

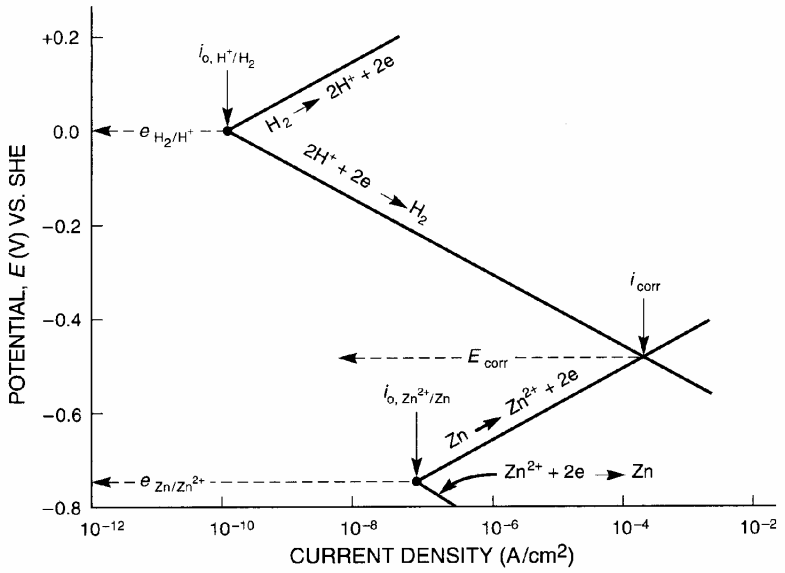

FIGURE 3.7 Polarization of anodic and cathodic half-cell reactions for zinc in acid solution to give a mixed potential, E_{corr}, and a corrosion rate (current density), i_{corr}. *(From M. G. Fontana,* Corrosion Engineering, *3rd ed., McGraw-Hill, New York, p. 457, 1986. Reprinted by permission, McGraw-Hill Book Company.)*

Effect of Exchange Current Density:

The exchange current density often outweighs the thermodynamic driving force in determining the rate of reaction. This is shown for the example of Fe and Zn. The half cell potential for the anodic oxidation of Fe is about –0.44V, while for Zn it is about –0.76V. Therefore Zn should corrode before Fe. Figure 3.8. shows the polarization diagrams for Zn (dashed lines) and Fe (solid lines). One can see that the current density at the corrosion potential for Fe is larger than the current density for Zn at the respective potential. Therefore Zn corrodes slower than Fe, although it has the more negative E_{corr}. Both i_{corr} and E_{corr} are used in corrosion protection of iron with a Zn coating, as the Zn starts to corrode first (E_{corr}), and the corrosion is much slower than that of Fe (i_{corr}).

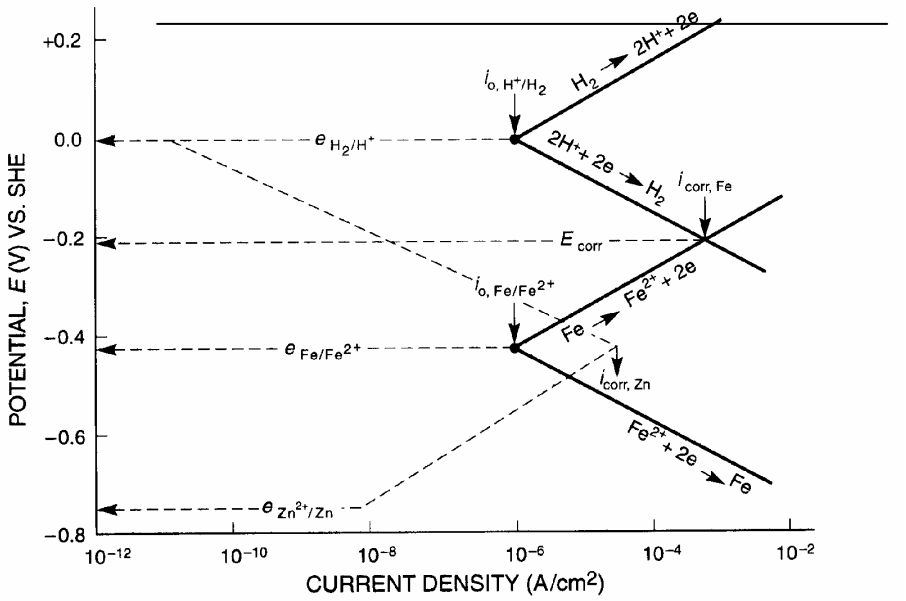

FIGURE 3.8 Comparison of electrochemical parameters for iron and zinc in acid solution, demonstrating the importance of i_o on determination of corrosion rates. Dashed lines represent lines from Figure 3.7 superimposed for comparison.

Effect of added oxidzer:

The driving force of corrosion is increased by the addition of a stronger oxidizer. In other words, when a redox system with a much more noble half cell potential is added to the system, the corrosion will increase. For example we consider the addition of Fe^{3+}/Fe^{2+} to an acid solution. Figure 3.9 shows the determination of the resulting mixed potential E_{corr} for the corroding metal M. The horizontal lines mark the half cell potentials for the three reactions that occur in the system. The dashed lines represent the total reduction rate and the total oxidation rate. Again E_{corr} is found where the total reduction rate equals the total oxidation rate. In figure 3.10 the determination of the anodic oxidation rate (i_{corr}) is shown for the same system as in figure 3.9. As the oxidation of M is the only oxidation reaction, i_{corr} equals the sum of the two cathodic reduction reactions $i(Fe^{3+} \rightarrow Fe^{2+})$ and $i(H^+ \rightarrow H_2)$.

Figure 3.9 shows that the added oxidizer only has an effect, when its exchange current density i_0 is large. With a low i_0 as shown in figure 3.11 there is no increase in the oxidation due to the added oxidizer, as the total rate of reduction is only due to $i(H^+ \rightarrow H_2)$ in this case.

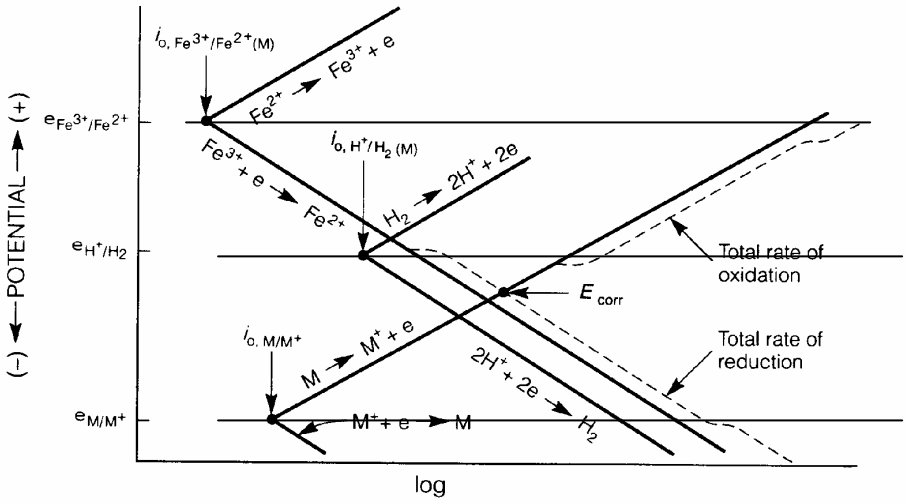

FIGURE 3.9 Determination of the mixed potential E_{corr} for a corroding metal M exposed to acid solution with a second oxidizer, Fe^{3+}/Fe^{2+}, present. *(From M. G. Fontana,* Corrosion Engineering, *3rd ed., McGraw-Hill, New York, p. 466, 1986. Reprinted by permission, McGraw-Hill Book Company.)*

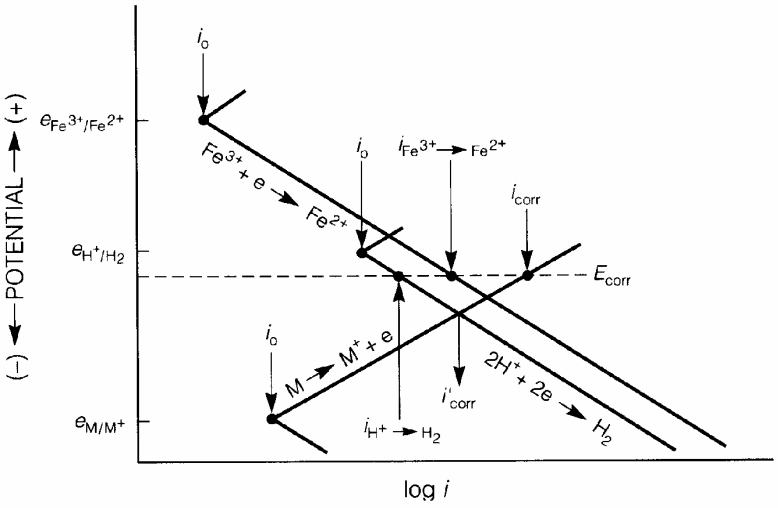

FIGURE 3.10 Rates of reduction ($i_{Fe^{3+} \rightarrow Fe^{2+}}$ and $i_{H^+ \rightarrow H_2}$) and oxidation (i_{corr}) from Figure 3.8 *(From M. G. Fontana,* Corrosion Engineering, *3rd ed., McGraw-Hill, New York, p. 467, 1986. Reprinted by permission, McGraw-Hill Book Company.)*

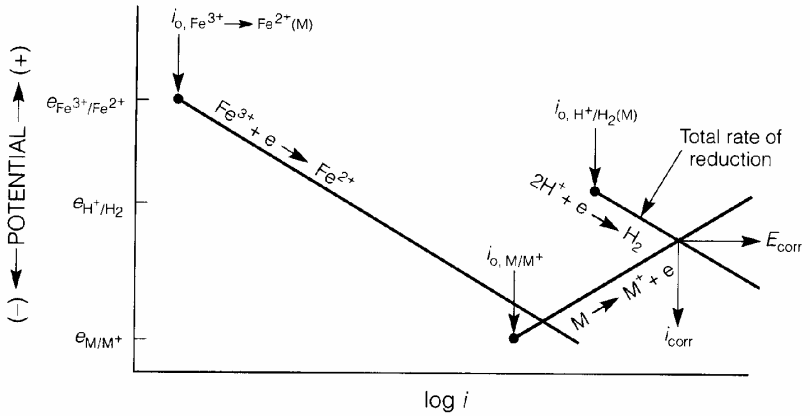

FIGURE 3.11 No effect on corrosion when oxidizer of low i_o is added to an acid solution. *(From M. G. Fontana,* Corrosion Engineering, *3rd ed., McGraw-Hill, New York, p. 467, 1986. Reprinted by permission, McGraw-Hill Book Company.)*

Cathodic and Anodic Polarization:

When an excess of electron flow is applied to a system with a current density of $i_{appl,\ c}$, the electrode potential shifts negatively from E_{corr} to E, which can be written as $\varepsilon_c = E - E_{corr}$. This leads to a decrease in i_a and an increase in i_c. As we still need an equal charge flow we can calculate $i_{appl,\ c} = i_c - i_a$. This is shown in figure 3.14a. A similar approach is valid for anodic polarization.

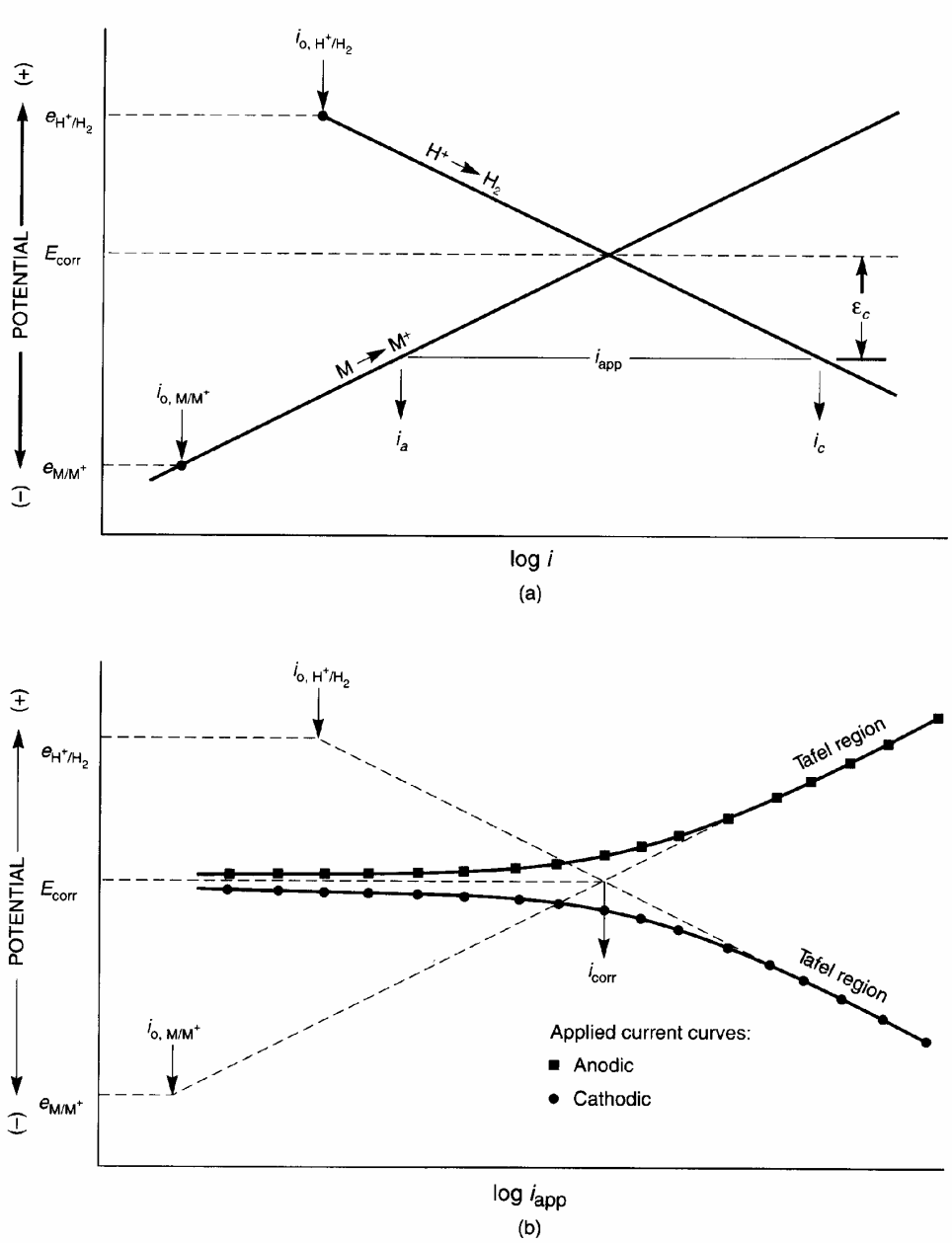

FIGURE 3.14 (a) Current density, i_{app}, applied to corroding electrode of E_{corr} and i_{corr}, causing cathodic overvoltage of ε_c; (b) simulated experimental polarization curves derived from (a).

In figure 3.14 b the data points represent $i_{appl,\ c}$ and $i_{appl,\ a}$, for cathodic and anodic polarization, respectively. With high ε_c and ε_a $i_{appl,\ c}$ and $i_{appl,\ a}$ are large and the points coincide with the tafel plots, whereas with lower ε_c and ε_a the measured points start to deviate from the

theoretical behaviour. As can be seen in figure 3.14b one can get i_{corr} and i_0 for the two half cell reactions by extrabolation of the linear part, where Tafel behaviour is observed. While this usually works good for the cathodic part, one usually does not get Tafel behaviour from measurements of the anodic part, as shown in figure 3.15. But one can calculate the anodic part from the cathodic measurements.

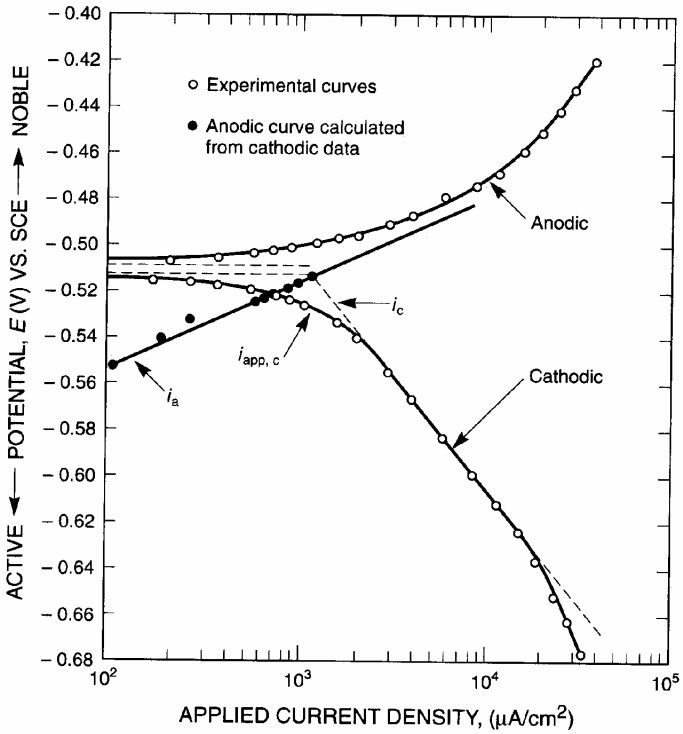

FIGURE 3.15 Experimental polarization curves for 1080 steel in deaerated 1 *N* H_2SO_4. β_c = –98 mV, β_a=38 mV (derived from cathodic data), i_{corr} = 1180 μA/cm². *(From R. Bandy and D. A. Jones,* Corrosion, *Vol. 32, p. 126, 1976. Reprinted by permission National Association of Corrosion Engineers.)*

An additional problem in interpreting measured data is the effect of concentration polarization. This brings significant additional deviation from Tafel behaviour as shown in figure 3.16.

Only at the lowest pH, which corresponds to the highest H^+ concentration, a nice linear part is observed in figure 3.16. With increasing pH (decreasing H^+ concentration) the experiment is mainly determined by the concentration polarization. At higher pH hydrogen evolution by direct reduction of water occurs $2H_2O + 2e^- \rightarrow H_2 + 2OH^-$, which again is linear following Tafel behaviour, as there is of course a very high concentration of water present.

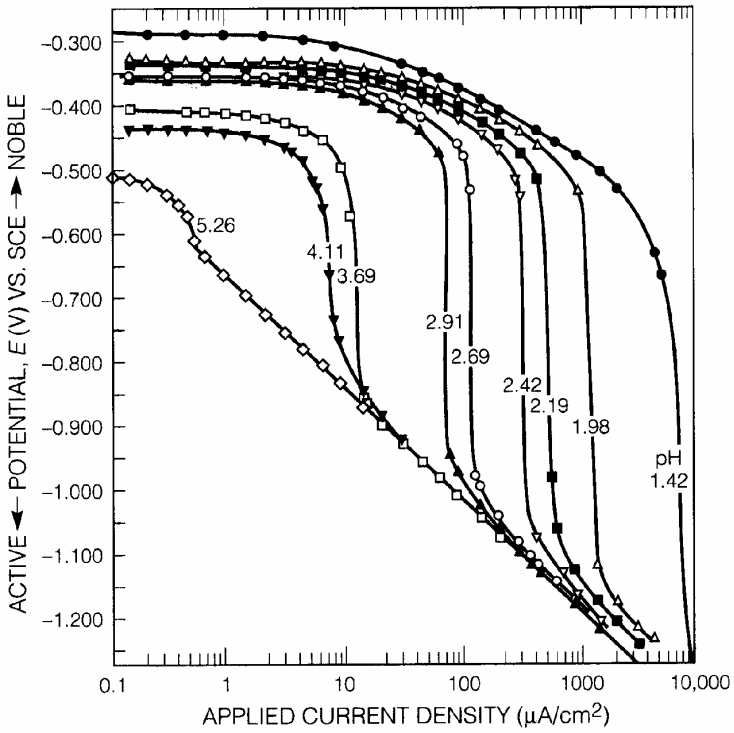

FIGURE 3.16 Cathodic polarization of pure iron in deaerated 4% NaCl. *(From M. Stern,* J. Electrochem. Soc., *Vol. 102, p. 609, 1955. Reprinted by permission, The Electrochemical Society.)*

Passivity

Passivity is defined as corrosion resistance due to formation of thin surface films under oxidizing conditions with high anodic polarization. For example Fe is passivated in concentrated nitric acid. But in diluted nitric acid Fe is dissolved, or when the passive film is scratched, Fe starts to dissolve, too. This is shown in the following figure.

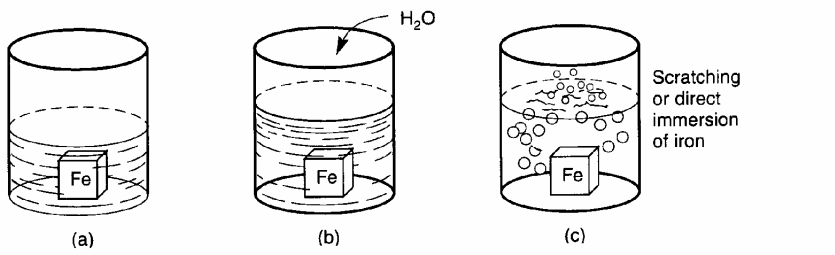

Fe only passivates in extremely oxidizing environments. The reason is the potential an pH range where iron oxides are thermodynamically stable. This can be seen in the Pourbaix diagram (see figure). Chromium (dashed lines and shaded area) passivates under less oxidizing conditions. But Cr has bad mechanical properties, therefore it is only used as an alloying element in Fe to make stainless steel (min 12% Cr). Ni (> 8%) further enhances corrosion resistance and improves mechanical properties by stabilizing the fcc phase of Fe.

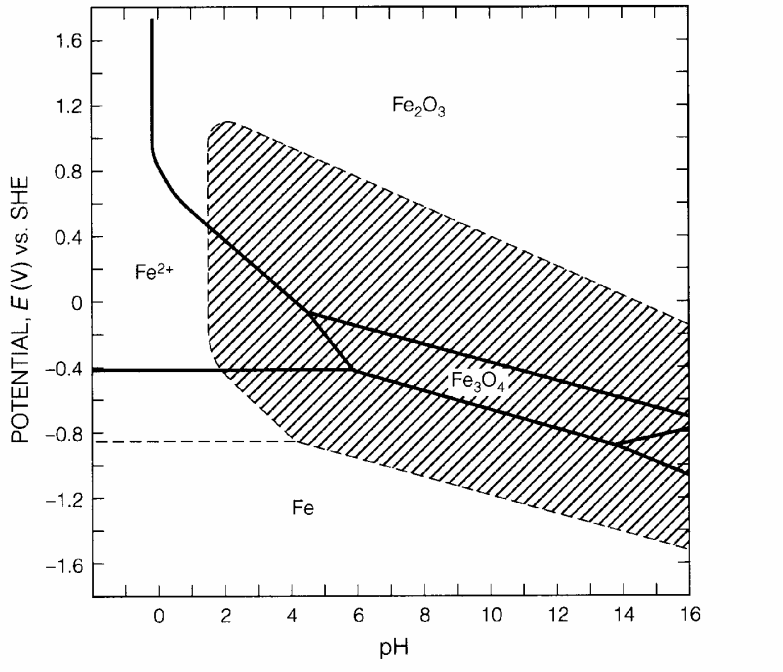

With increasing potential and anodic polarization passive metals show a distinct behaviour. At low potentials corrosion rates measured by anodic current density are high and increase with potential in the active state. Above the primary passive potential E_{pp} the passive film becomes stable and the corrosion rate decreases significantly. i_{pass} can be up to 10^6 times lower than i_{crit}, as indicated in figure 4.3.

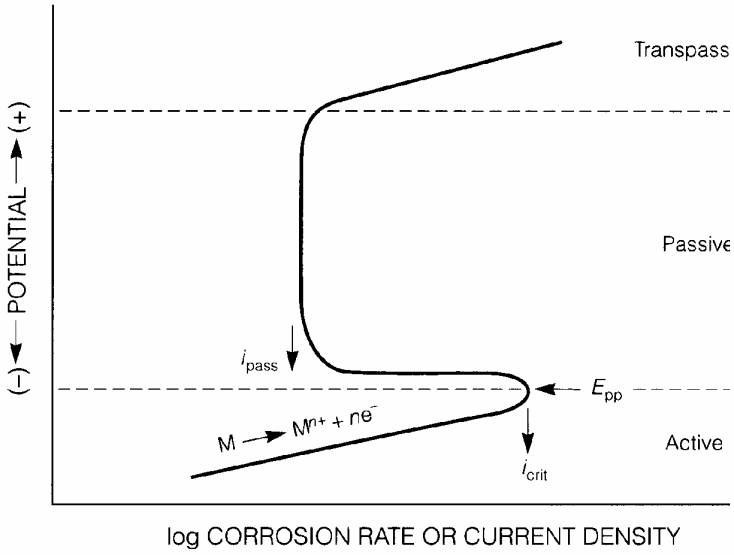

FIGURE 4.3 Schematic active–passive polarization behavior.

At very high potentials the passive to transpassive transition occurs and the corrosion rate increases again. For stainless steel this potential is near the oxygen evolution potential, where the Cr rich passive film is unstable, as can be seen in the Pourbaix diagram. Going to higher H^+ concentrations (higher acidity) and to higher temperatures leads to a decrease in the extend of the passive region, as shown in figure 4.4.

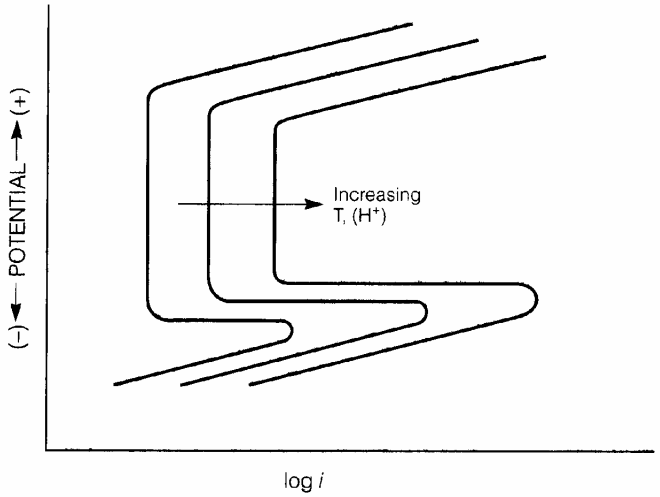

FIGURE 4.4 Effect of increasing acid concentration and temperature on passivity.

Oxidizer Concentration Effects:

An increase in the oxidizer concentration increases the potential of the redox half cell reaction according to the Nernst equation. Taking mixed potential theory into account one can depict the effect of oxidizer concentration as shown in figure 4.5. The corrosion rate changes with

increasing oxidizer concentration from 1 to 8. The corresponding corrosion rates (current densities) are labeled A through F.

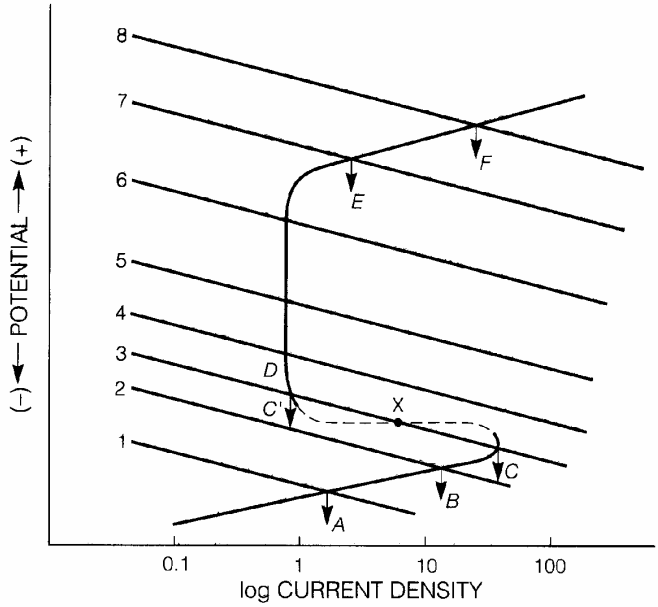

FIGURE 4.5 Effect of oxidizer concentration on corrosion of an active–passive alloy.

From figure 4.5 one can make another plot with corrosion rate versus oxidizer concentration. In this case (figure 4.6) one can clearly see a hysteresis effect. This borderline passivity is an instable state, where any surface disturbance (scratching, stress, etc) will destabilize the passive film.

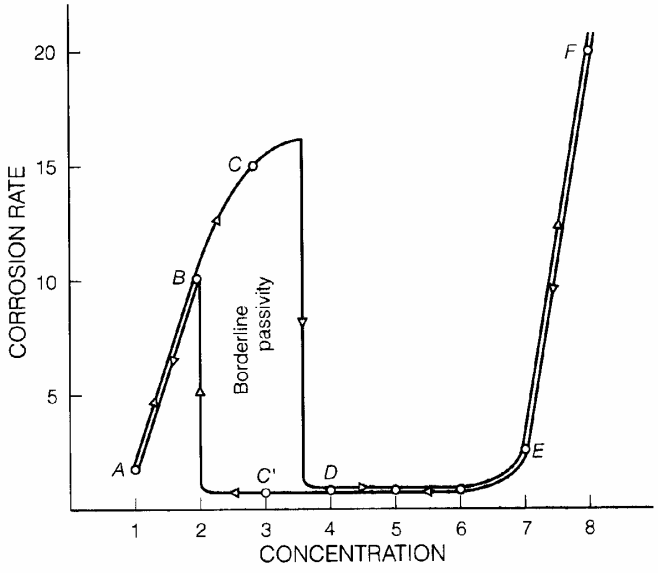

FIGURE 4.6 Effect of oxidizer concentration on corrosion rate in an active–passive metal or alloy.

Solution Velocity Effects:

In a dilute salt solution (e.g. seawater) there is under deaerated conditions only one cathodic

reduction reaction available:

$$2H_2O + 2e^- \rightarrow H_2 + 2OH^-$$

and therefore the metal corrodes in the active state. But the rate of hydrogen evolution is small and therefore the corrosion rate is small, too. If the solution becomes aerated, reduction of dissolved oxygen

$$O_2 + 2H_2O + 4e^- \rightarrow 4OH^-$$

starts to predominate as shown by line 1 in figure 4.7. In this case one has borderline passivity.

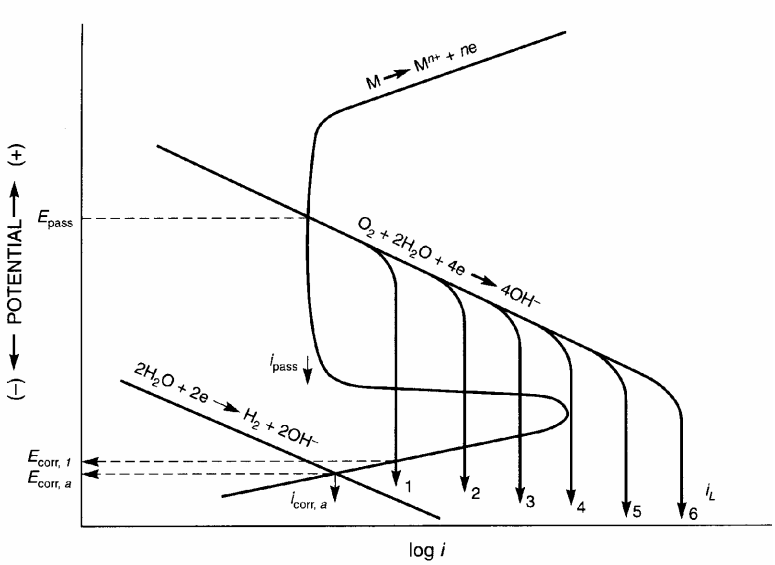

FIGURE 4.7 Effect of deaeration, aeration, and stirring on corrosion of active–passive stainless steel in neutral saltwater.

But agitation of the solution leads to an increase in the limiting diffusion current from 1 to 6, and the system gets in the passive state. In figure 4.8 a the corrosion rate from figure 4.7 is plotted against the solution velocity (agitation). For comparison figure 4.8 b shows the same plot for a metal that does not form a passive film. There the corrosion only shifts from concentration to activation control.

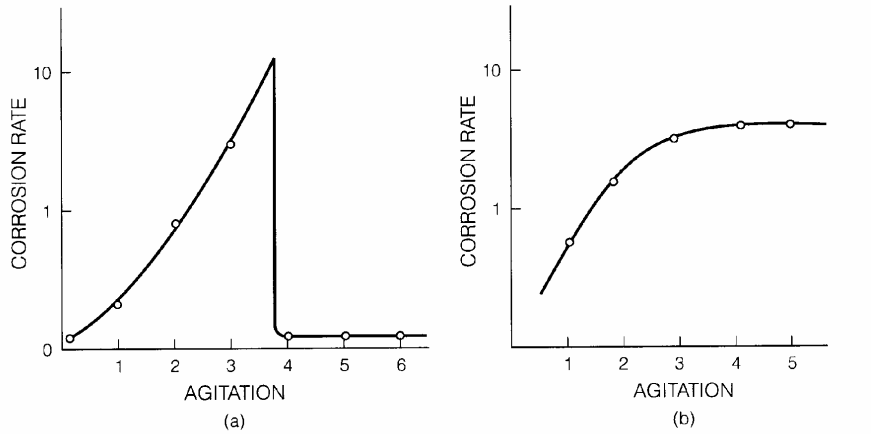

FIGURE 4.8 Effect of stirring or solution velocity on corrosion rate for (a) active–passive stainless steel, derived from Figure 4.6, and (b) normal active metal, reproduced from Figure 3.13b.

reduction reaction available:

$$2H_2O + 2e^- \rightarrow H_2 + 2OH^-$$

and therefore the metal corrodes in the active state. But the rate of hydrogen evolution is small and therefore the corrosion rate is small, too. If the solution becomes aerated, reduction of dissolved oxygen

$$O_2 + 2H_2O + 4e^- \rightarrow 4OH^-$$

starts to predominate as shown by line 1 in figure 4.7. In this case one has borderline passivity.

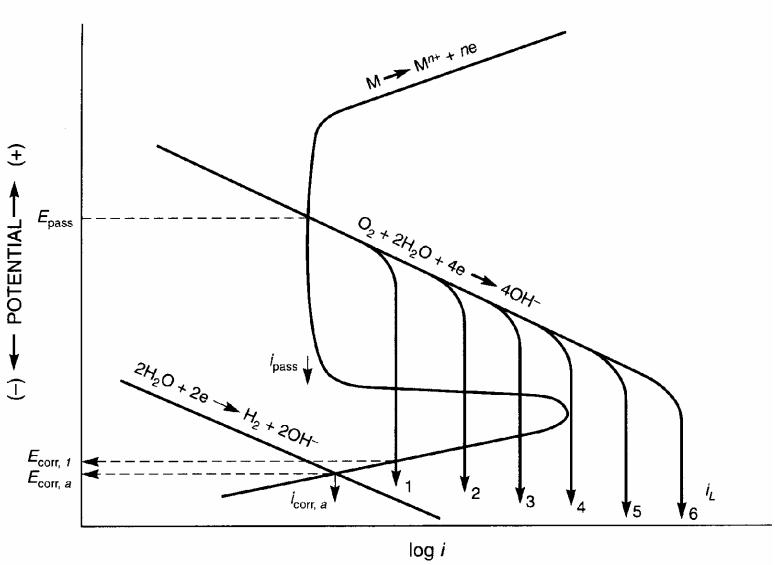

FIGURE 4.7 Effect of deaeration, aeration, and stirring on corrosion of active–passive stainless steel in neutral saltwater.

But agitation of the solution leads to an increase in the limiting diffusion current from 1 to 6, and the system gets in the passive state. In figure 4.8 a the corrosion rate from figure 4.7 is plotted against the solution velocity (agitation). For comparison figure 4.8 b shows the same plot for a metal that does not form a passive film. There the corrosion only shifts from concentration to activation control.

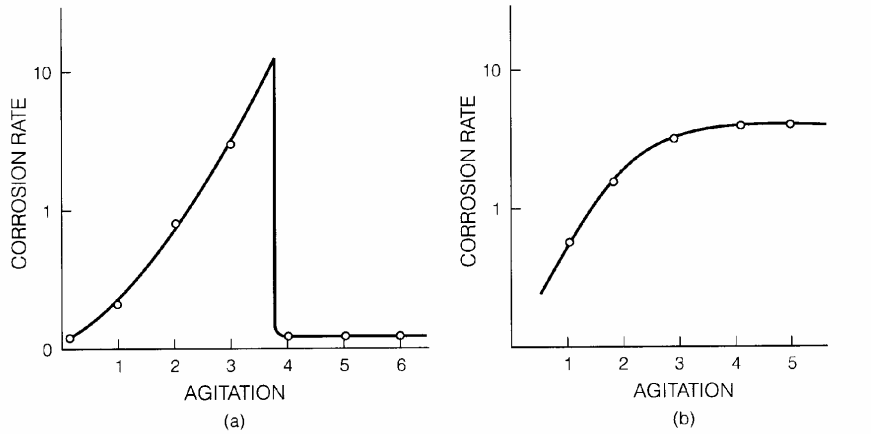

FIGURE 4.8 Effect of stirring or solution velocity on corrosion rate for (a) active–passive stainless steel, derived from Figure 4.6, and (b) normal active metal, reproduced from Figure 3.13b.

Experimental Apparatus and Procedures:

Potentiostatic and potentiodynamic procedures are used to measure the anodic polarization behaviour of metals. A potentiostat automatically adjusts the applied polarizing current to control potential between the working electrode (WE) and the reference electrode (REF). A schematic of such a system is shown in figure 4.10.

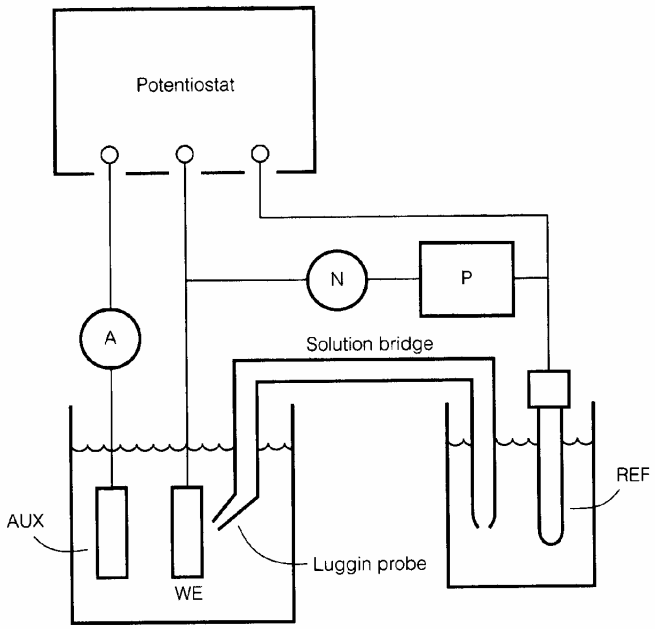

FIGURE 4.10 Controlled potential circuitry utilizing a potentiostat.

The current I polarizes the WE to the prescribed potential with respect to REF. In this setup no current passes through the REF, which has a constant potential. The result of such a measurement is shown in figure 4.11.

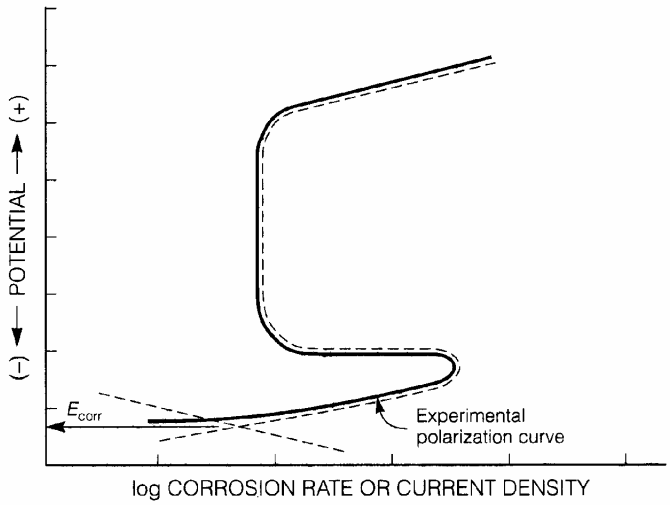

FIGURE 4.11 Polarization of an active–passive alloy with controlled (potentiostatic) potential.

In the measurment the potential is increased from E_{corr} in the active state in steps. After a step

the current is recorded and so on. In a potentiodynamic setup the potential is continually increased, while the current is continually measured at the same time. The result is the same as in the potentistatic experiment. An example of a real system is shown in figure 4.12. The potentiostatic polarizatzion cures of Fe and Fe-10.5Cr are shown.

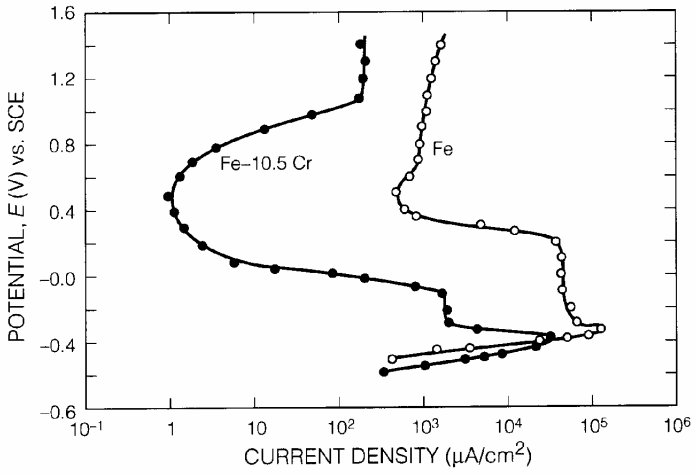

FIGURE 4.12 Potentiostatic anodic polarization of pure iron and iron-10.5% chromium alloy. *(Adapted from Steigerwald and Greene[6].)*

Anodic polarization curves are affected by the rate of polarization (scan rate in Vs^{-1}) (see figure 4.13) and by differences in the measured samples (see figure 4.14).

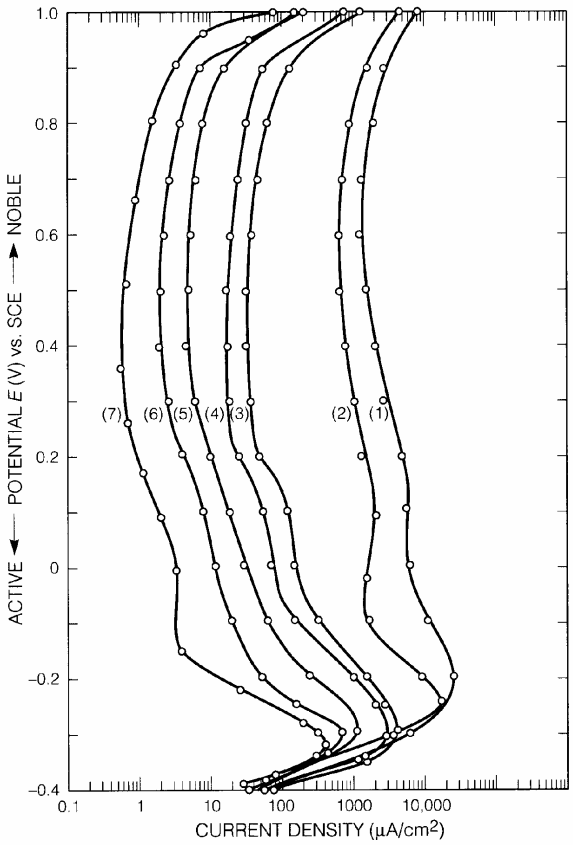

FIGURE 4.13 Effect of decreasing polarization rate (1) to (7) on potentiostatic anodic polarization curves for AISI 304 stainless steel in deaerated 1*N* H_2SO_4 at 25°C. *(From N. D. Greene and R. B. Leonard,* Electrochim. Acta, *Vol. 9, p. 45, 1964. Reprinted by permission, Pergamon Press.)*

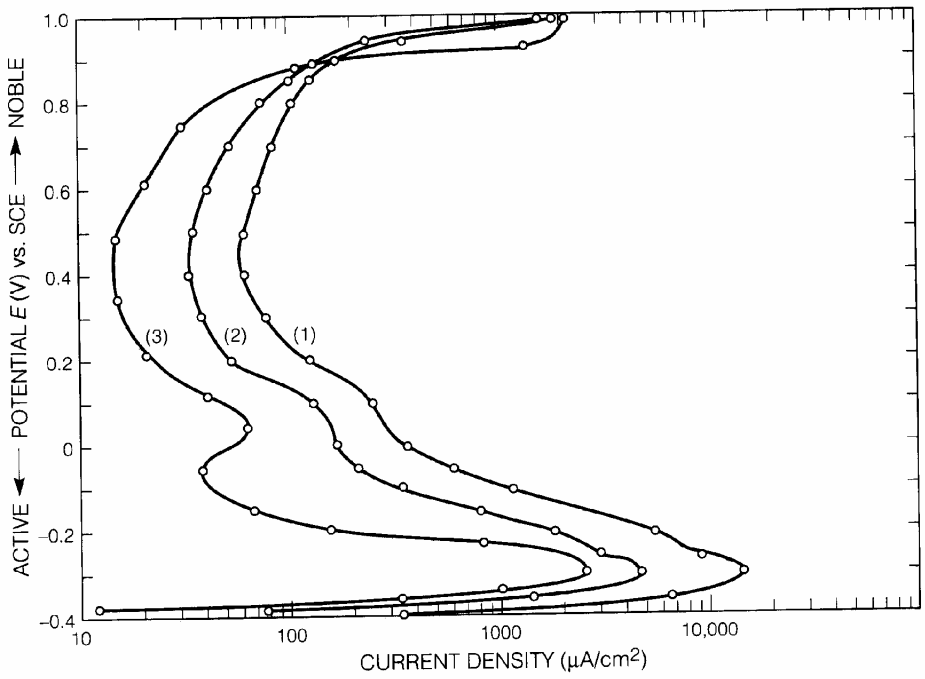

FIGURE 4.14 Effect of differing heats, (1) and (3), and differing specimens from the same heat, (1) and (2), on potentiostatic anodic polarization curves for AISI 304 stainless steel in deaerated 1*N* H_2SO_4 at 25°C; traverse rate 12 V/h. *(From N. D. Greene and R. B. Leonard,* Electrochim, Acta, *Vol. 9, p. 45, 1964. Reprinted by permission, Pergamon Press.)*

Potentiodynamic anodic polarization curves are used to judge corrosion resistance of alloys and the corrosivity of solutions. The experiments only need a couple of minutes. Potentiostatic measurements need a few hours, which is still short in comparison to the weeks or months needed for conventional testing. For example one can use the data to choose an alloy for different environments. The plots are shown in figure 4.16.

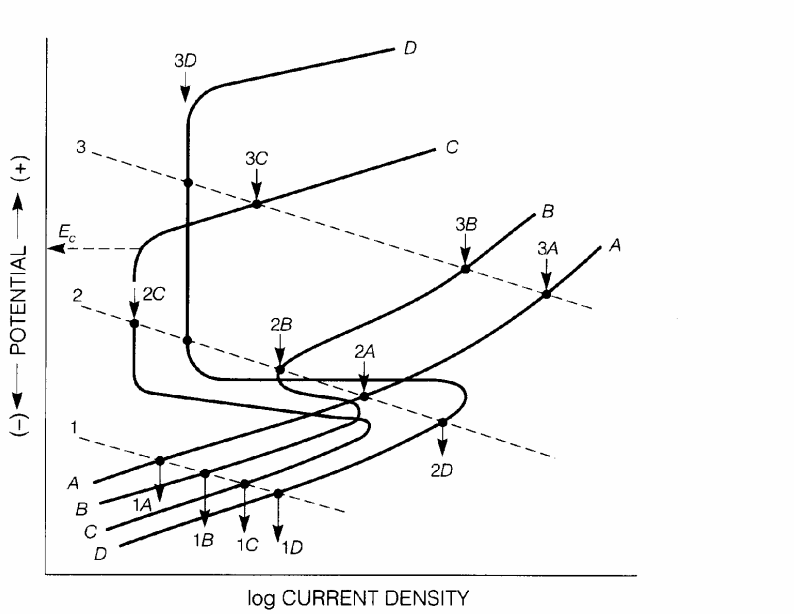

FIGURE 4.16 Schematic anodic polarization curves for hypothetical alloys *A, B, C,* and *D,* illustrating evaluation in various chemical conditions: 1, reducing; 2, moderately oxidizing; 3, highly oxidizing.

There are 5 parameters that may be used to judge an alloy:

1. In the active state, corrosion rate is proportional to the anodic current density whether or not the alloy is of the active-passive type.
2. The current density (rate) of reduction must exceed the critical current density for passivation to ensure low corrosion rate in the passive state.
3. Borderline passivity should be avoided in which either the active or the passive state may be stable.
4. Breakdown of the passive film in oxidizing conditions due to transpassivity or initiation of localized corrosion should be avoided.
5. The passive state in oxidizing conditions is essential for corrosion resistance, but reasonably small variations in the passive current density may not be significant.

A real world example is shown in figure 4.17. Hastealloy B is Ni-25Mo, C is Ni-15Cr-15Mo-5Fe and C-276 has low Si and C impurities. One can see that the latter has the best passive region. For use in the active region one would use alloy B as it does not contin expansive Cr. Apparently is the anodic polarization very sensitive to impurities.

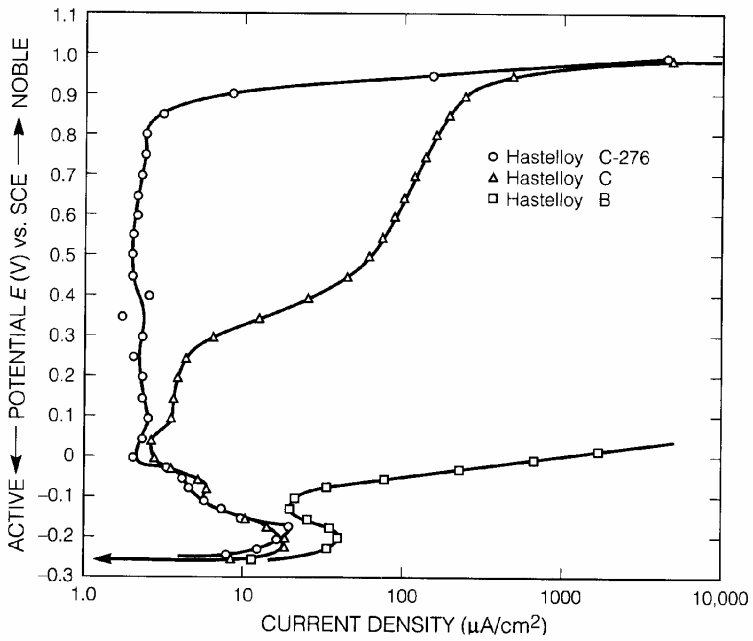

FIGURE 4.17 Comparison of potentiostatic anodic polarization of nickel alloys in 1 *N* H_2SO_4, ambient temperature. *(By courtesy of F. G. Hodge, Haynes International.)*

The influence of the solution is shown in figure 4.18. In this case one can see that the addition of chloride to the solution has a profound effect on the anodic polarization of steel, whereas hastealloy C is less affected. But in chloride free solutions the steel performs better.

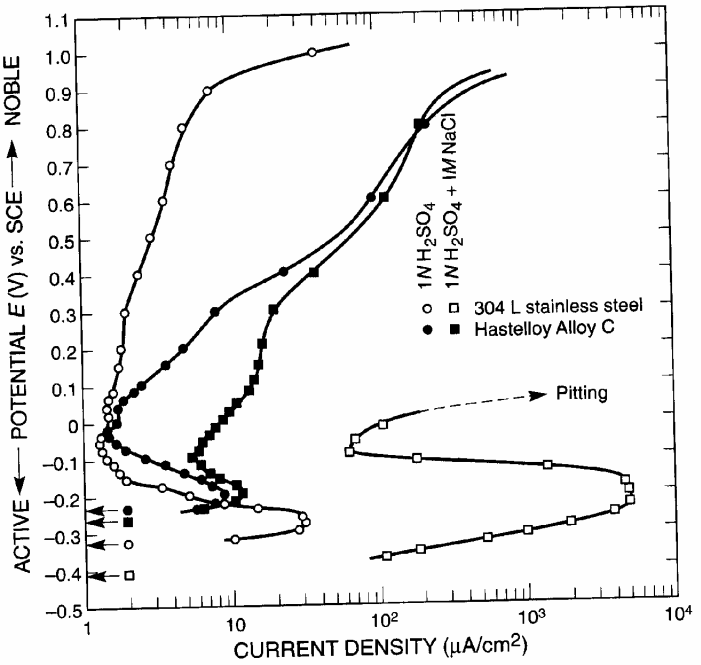

FIGURE 4.18 Effect of added chloride on potentiostatic anodic polarization of stainless steel and nickel Alloy C in sulfuric acid. *(Adapted from Green and Judd.[10])*

There are of course limitations to the data achieved by potentiodynamic anodic polarization. Under plant conditions additional processes can occur that influence the corrosion resistance of a material. Passive current density and corrosion rates can change over time. Therfore only qualitative predictions can be made. Then more extensive in-plant exposure tests are necessary.

Anodic Protection:

If an active passive metal is maintained in the passive region with a potentiostat its corrosion rate will be low at i_{pass}. With the electrical parts scaled up to plant size this is called anodic protection. The metal needs to have a broad passive region, as a wrong potential outside of the passive region would lead to increased corrosion. The method so far is only used for storage tanks for very corrosive acids (e.g. sulfuric acid (steel), phosphoric acid (stainless steel) and nitric acid (nickel)).

Properties of Passive Films:

The properties of passive films are unfortunately rather elusive. While potentiodynamic anodic polarization contains a lot of information, it is not possible to delineate the mechanism of the transition to the transpassive state. Passivity has been investigated for about 140 years,

but still not much is known about the structure of the films. It is clear that the films contain some water and most films are more likely hydroxides and not oxides. Surface analysis of the films is a problem, as the morphology of the film can change, when it is transferred into the vacuum. Water bound in the structure can be lost and this may lead to or change crystallization. Due to the fact that passive films are very thin most of them show semiconducting behaviour. For some cases it has been shown that the passive film is amorphous (e.g. Fe, Al). It has been shown recently [Mamun A, Schennach R, Parga JR, Mollah MYA, Hossain MA and Cocke DL Electrochimica Acta, **46** (22) 3343 (2001)] that oxygen evolution can initiate crystallization of the passive film on zirconium, which coincides with the passive transpassive transition.

Galvanic and Concentration Cell Corrosion

A galvanic cell is formed, when two different metals are connected electrically, while both are immersed in an electrolyte. In this case one of the two is corroded preferentially by galvanic corrosion. When different solution concentrations are present on the same metal surface, a concentration cell is formed, which leads to preferential corrosion, too. When attack on the junction of two dissimilar alloys is limited to one of the two, one usually has galvanic corrosion. The preferentially corroded alloy is the anode in the galvanic couple and the unattacked alloy is the cathode. The cathode may be damaged by hydrogen or by cathodic polarization out of the passive into the active zone.

Any metal or alloy has a unique corrosion potential E_{corr} immersed in a corrosive electrolyte. When two metals are coupled, the one with the more negative E_{corr} will lose electrons, which leads to an increased corrosion rate. The anodic dissolution, or corrosion reaction is

$$M \rightarrow M^{n+} + ne^-$$

for the active metal. The rate for the more noble metal N is decreased due to the excess electrons from M.

$$N \rightarrow N^{m+} + me^-$$

N is the cathode of the galvanic cell and M is the anode. The corrosion rate decrease in the cathode is the basis of cathodic protection by a sacrificial anode.

The corrosion potentials of different metals and alloys in a specified electrolyte give a galvanic series. Such a series gives a qualitative prediction, which alloy or metal will corrode first in a galvanic couple. But the quantitative corrosion rate can not be predicted from this series, as the influences of solution velocity and temperature are neglected. And the series is not necessarily the same for a different electrolyte, although people sometimes try to draw conclusions from the seawater series for different electrolytes.

Area Effects:

A large ratio of the cathode to anode surface area should be avoided. For small anodes the galvanic attack is concentrated and penetration of the attack through the metal is faster. A larger anode surface will give a more uniform attack and will slow down the rate of penetration. A classic example are storage tanks with new stainless steel bottoms and coated sides made of normal steels. The galvanic corrosion penetrated the sides quickly, due to small

Galvanic and Concentration Cell Corrosion

A galvanic cell is formed, when two different metals are connected electrically, while both are immersed in an electrolyte. In this case one of the two is corroded preferentially by galvanic corrosion. When different solution concentrations are present on the same metal surface, a concentration cell is formed, which leads to preferential corrosion, too. When attack on the junction of two dissimilar alloys is limited to one of the two, one usually has galvanic corrosion. The preferentially corroded alloy is the anode in the galvanic couple and the unattacked alloy is the cathode. The cathode may be damaged by hydrogen or by cathodic polarization out of the passive into the active zone.

Any metal or alloy has a unique corrosion potential E_{corr} immersed in a corrosive electrolyte. When two metals are coupled, the one with the more negative E_{corr} will lose electrons, which leads to an increased corrosion rate. The anodic dissolution, or corrosion reaction is

$$M \rightarrow M^{n+} + ne^-$$

for the active metal. The rate for the more noble metal N is decreased due to the excess electrons from M.

$$N \rightarrow N^{m+} + me^-$$

N is the cathode of the galvanic cell and M is the anode. The corrosion rate decrease in the cathode is the basis of cathodic protection by a sacrificial anode.

The corrosion potentials of different metals and alloys in a specified electrolyte give a galvanic series. Such a series gives a qualitative prediction, which alloy or metal will corrode first in a galvanic couple. But the quantitative corrosion rate can not be predicted from this series, as the influences of solution velocity and temperature are neglected. And the series is not necessarily the same for a different electrolyte, although people sometimes try to draw conclusions from the seawater series for different electrolytes.

Area Effects:

A large ratio of the cathode to anode surface area should be avoided. For small anodes the galvanic attack is concentrated and penetration of the attack through the metal is faster. A larger anode surface will give a more uniform attack and will slow down the rate of penetration. A classic example are storage tanks with new stainless steel bottoms and coated sides made of normal steels. The galvanic corrosion penetrated the sides quickly, due to small

defects in the protective coating which are unavoidable. The new tanks started to leak already after a few months. The problem is shown in figure 6.2.

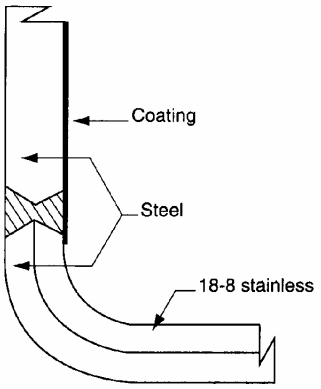

FIGURE 6.2 Painted steel storage tank which developed penetration through a coating due to galvanic coupling to a new stainless steel bottom. *(From M. G. Fontana,* Corrosion Engineering, *3rd ed., McGraw-Hill, New York, pp. 46–49, 1986. Reprinted by permission, McGraw-Hill Book Company.)*

Prevention:

The best way to prevent galvanic corrosion is to eliminate the galvanic couple by design, whenever possible. Using materials with similar E_{corr} reduces the driving force for galvanic corrosion drastically. Insulated flanges can be used to avoid a galvanic couple (figure 6.3).

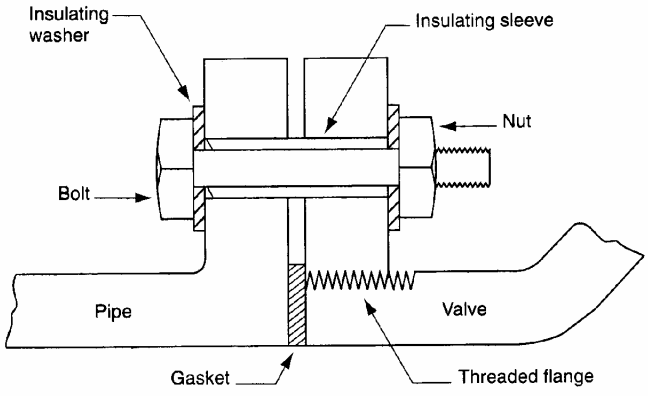

FIGURE 6.3 Insulated flange to eliminate a galvanic couple. *(From M. G. Fontana,* Corrosion Engineering, *3rd ed., McGraw-Hill, New York, pp. 46–49, 1986. Reprinted by permission, McGraw-Hill Book Company.)*

But soluble corrosion products can be deposited on active metals downstream and form in situ galvanic couples. If the galvanic couple cannot be avoided a large anode area and a large anode thickness should be used. The anode can also be designed foe easy replacement. Coating is usually not advisable (example with the tanks). If coating is applied it should be put on the cathode to prevent the cathodic reaction. In this case small defects in the coating do not have such severe effects as on the anode.

Fundamental Aspects:

Corroding Metal – Inert Metal Couple:

When zinc is coupled to platinum in dilute acid solutions experiments show that,

1. the corrosion potential of Zn is shifted to a more noble value
2. the corrosion rate of Zn is increased and
3. the hydrogen evolution on Zn is reduced.

These effects are due to cathode and anode polarization within the couple, as shown in figure 6.4.

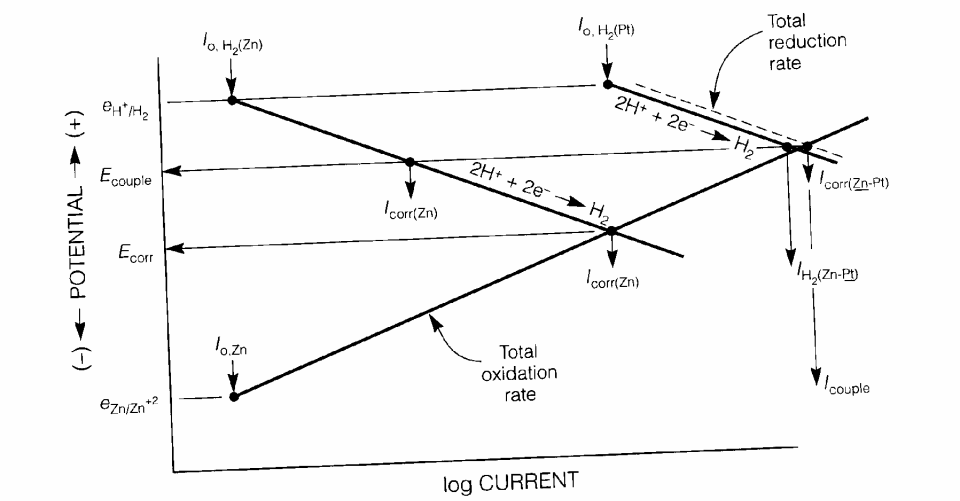

FIGURE 6.4 Schematic polarization in a galvanic couple between zinc and platinum in dilute acid solution.

The electrons from the anodic reaction (Zn Zn2+ + 2e-) flow to Pt until both electrodes are at the same potential E_{couple}, which is a similar effect as an impressed current i_{app}, shown in figure 3.14. The exchange current density of the hydrogen evolution reaction also affects the galvanic cell as shown in figure 6.5.

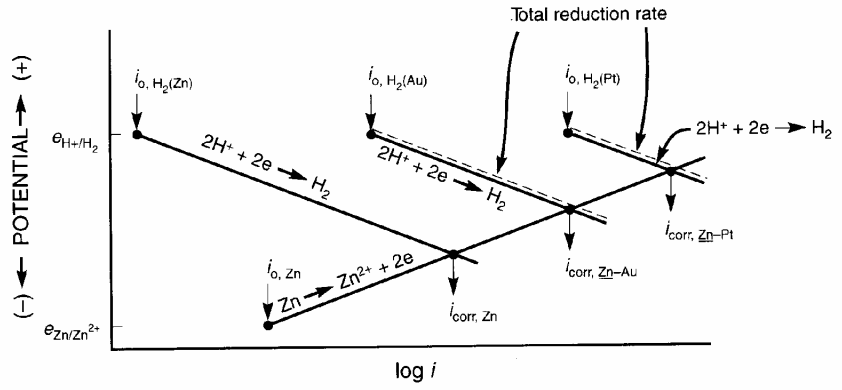

FIGURE 6.5 Effects of platinum and gold galvanically coupled to zinc in dilute acid solution.

Increasing the surface area of the cathode leads to an increase in the corrosion rate of the anode. As the current from the reduction reaction increases, the anodic oxidation reaction needs to increase too, to maintain a constant charge. The effect is schematically shown in figure 6.6.

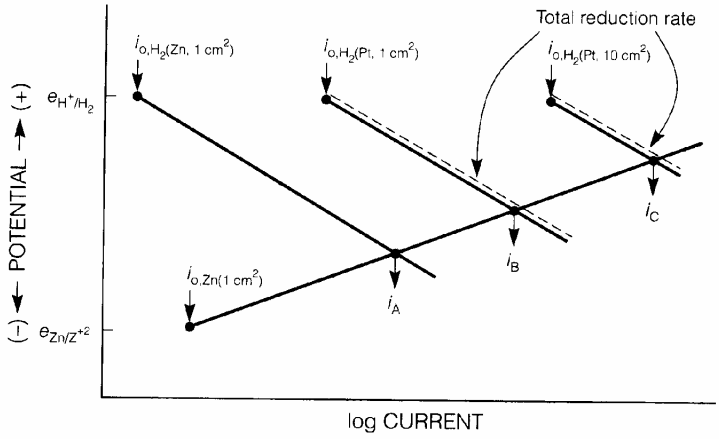

FIGURE 6.6 Effect of increased cathode surface area on the galvanic interaction between zinc and platinum in dilute acid solution.

Corroding Metal – Corroding Metal Couple:

Two metals M and N are corroding metals. M is the cathode metal and N is the anode metal. Again the coupled potential is found where the total reduction is equal to the total oxidation, as shown in figure 6.7.

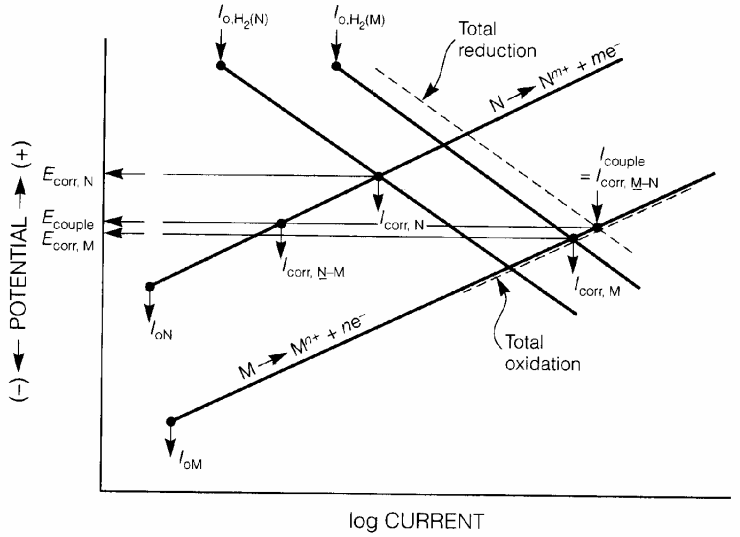

FIGURE 6.7 Schematic polarization in a galvanic couple between corroding metals M (anode) and N (cathode).

The potential of the couple always falls between the corrosion potentials of the two active metals. The rate of the metal with the more active E_{corr} is increased and the rate of the metal with the more noble E_{corr} is decreased. At breaks in a Zn coated steel, the Zn is galvanically corroded to protect the exposed steel cathodically.

Experimental Measurements:

A schematic of an experimental result is shown in figure 6.8. The dashed lines represent the half cell reactions defining the uncoupled corrosion potentials for anode and cathode. The solid lines represent data from a galvanic couple, where the couple potential is established when cathode and anode are polarized to equal potentials by the same current I_{couple}.

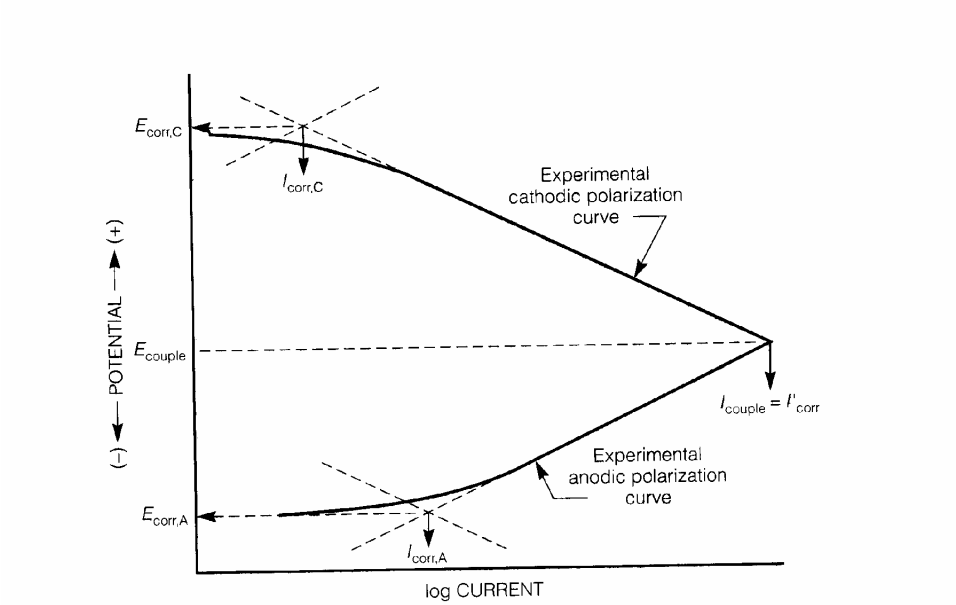

FIGURE 6.8 Schematic experimental polarization of anode and cathode in a galvanic couple.

For experimental measurements one uses a high surface area ratio cathode to anode (e.g. 12:1 in figure 6.9) and due to the large cathode area one does not need the auxiliary electrode, from polarization measurements.

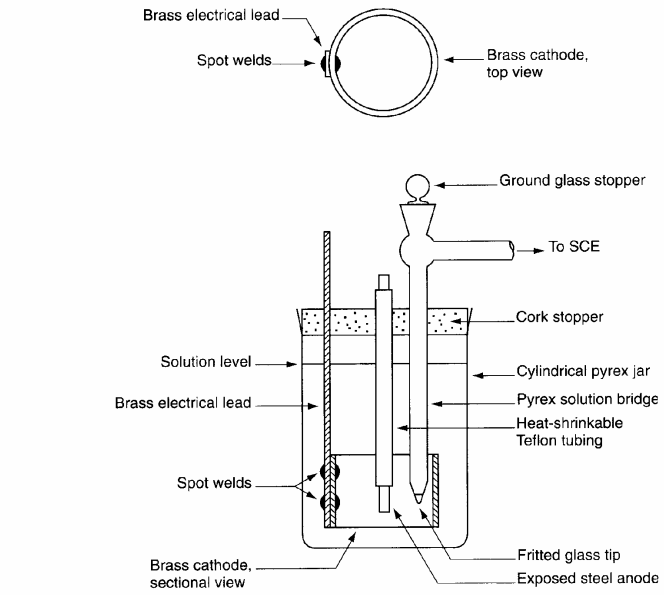

FIGURE 6.9 Cell for electrochemical study of steel anode, A, and brass cathode, C. *(From D. A. Jones,* Corrosion, *Vol. 40, p. 181, 1984. Reprinted by permission, National Association of Corrosion Engineers.)*

Experimental Measurements:

A schematic of an experimental result is shown in figure 6.8. The dashed lines represent the half cell reactions defining the uncoupled corrosion potentials for anode and cathode. The solid lines represent data from a galvanic couple, where the couple potential is established when cathode and anode are polarized to equal potentials by the same current I_{couple}.

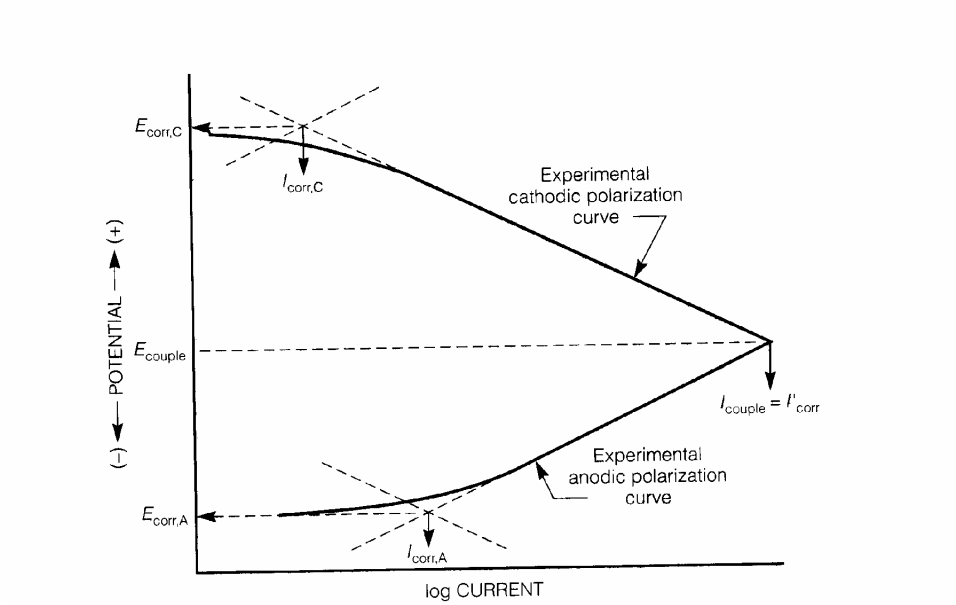

FIGURE 6.8 Schematic experimental polarization of anode and cathode in a galvanic couple.

For experimental measurements one uses a high surface area ratio cathode to anode (e.g. 12:1 in figure 6.9) and due to the large cathode area one does not need the auxiliary electrode, from polarization measurements.

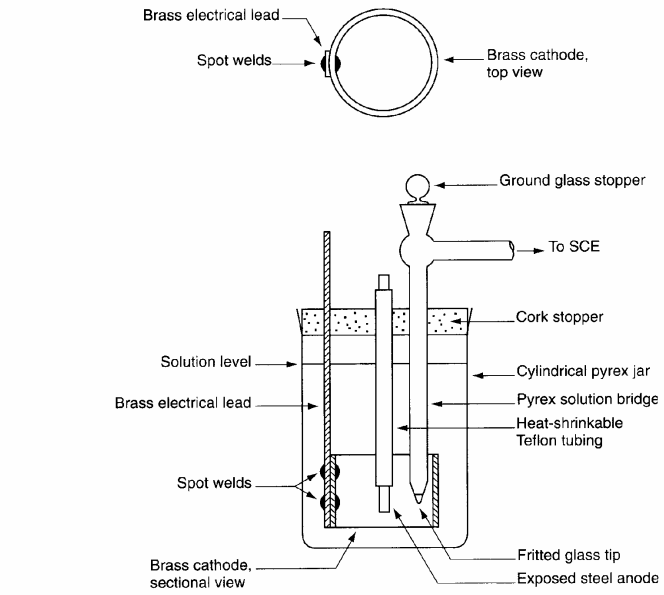

FIGURE 6.9 Cell for electrochemical study of steel anode, A, and brass cathode, C. *(From D. A. Jones,* Corrosion, *Vol. 40, p. 181, 1984. Reprinted by permission, National Association of Corrosion Engineers.)*

Results from the cell shown in figure 6.9 are depicted in figure 6.11. Different area ratios shown in the figure were simulated by moving the experimental cathodic curve to higher or lower values with respect to the anodic curve. The intersections of the cathodic and the anodic curves show the couple potentials for the different surface area ratios.

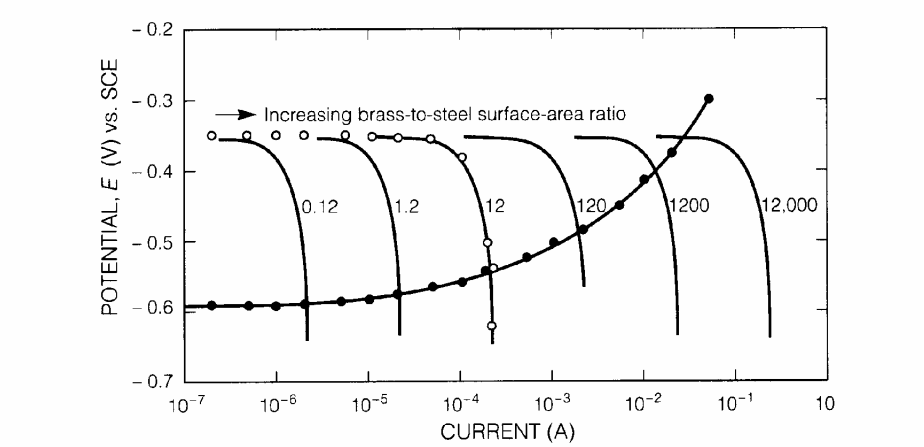

FIGURE 6.11 Experimental cathodic (○) and anodic (●) polarization curves in aerated 20% NaCl at room temperature for brass and steel, respectively, having surface area ratio of 12:1. Other surface area ratios simulated by moving cathodic curve with respect to the anodic curve. *(From D. A. Jones,* Corrosion, *Vol. 40, p. 181, 1984, Reprinted by permission, National Association of Corrosion Engineers.)*

The couple potentials graphically determined from figure 6.11 are shown as a function of the surface area ratio in the solid line in figure 6.12. The points in this figure are from actual experiments with the corresponding surface area ratio. One can see a rather good fit between experiment and theory.

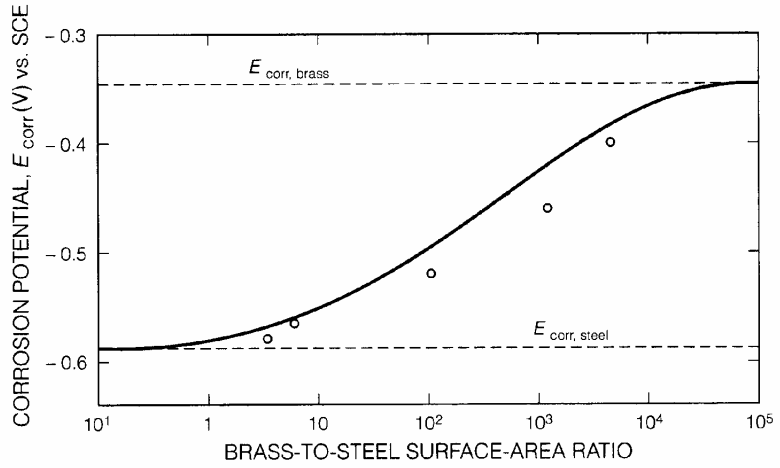

FIGURE 6.12 Graphically simulated couple potential (———) compared with experimental measurements (○) versus cathode/anode area ratio. *(From D. A. Jones,* Corrosion, *Vol. 40, p. 181, 1984. Reprinted by permission, National Association of Corrosion Engineers.)*

In principle one should be able to measure the coupled current by simply putting an ampere meter between the two electrodes. But due to the resistance of the ampere meter one gets a wrong current, as shown in figure 6.13. This problem can be avoided by using zero resistance ampere meters, which can be realized using a special electronic setup.

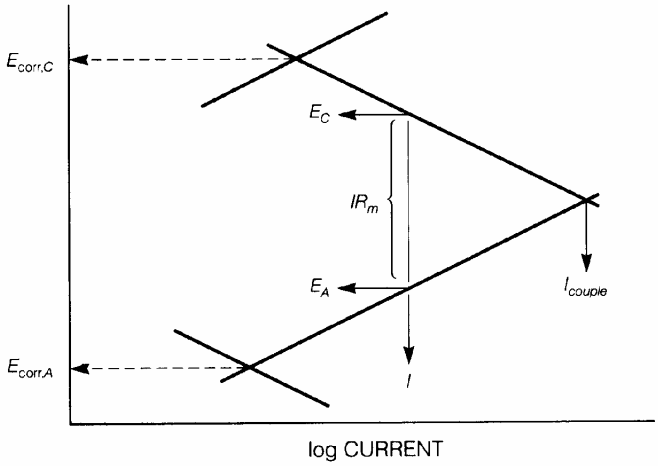

FIGURE 6.13 Separation of anode and cathode potentials when measuring galvanic current I with ammeter of resistance R_m.

The zero resistance ampere meter can be realized with the usual electrode setup combined with a potentiostat. In this case one can measure I_{couple} continuously and automatically. The measurement principle is shown in figure 6.14.

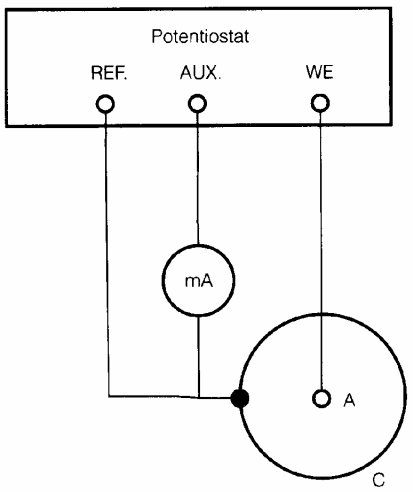

FIGURE 6.14 Potentiostatic zero resistance ammeter for continuous and automatic measurement of couple current at short circuit. *(From D. A. Jones,* Corrosion, *Vol. 40, p. 181, 1984. Reprinted by permission, National Association of Corrosion Engineers.)*

The potentiostat senses a difference between REF and WE and controls the difference at a preset value by automatically varying the current between WE and AUX. When WE and REF are shorted as shown in the figure the potentiostat will control the potential between cathode and anode at any specified value. If this value is zero the circuit will continuously and automatically read the I_{couple} at short circuit on the ampere meter. The result of such a measurement of short circuit current with time is shown in figure 6.15. In addition the effect of a dichromate inhibitor is shown in this figure.

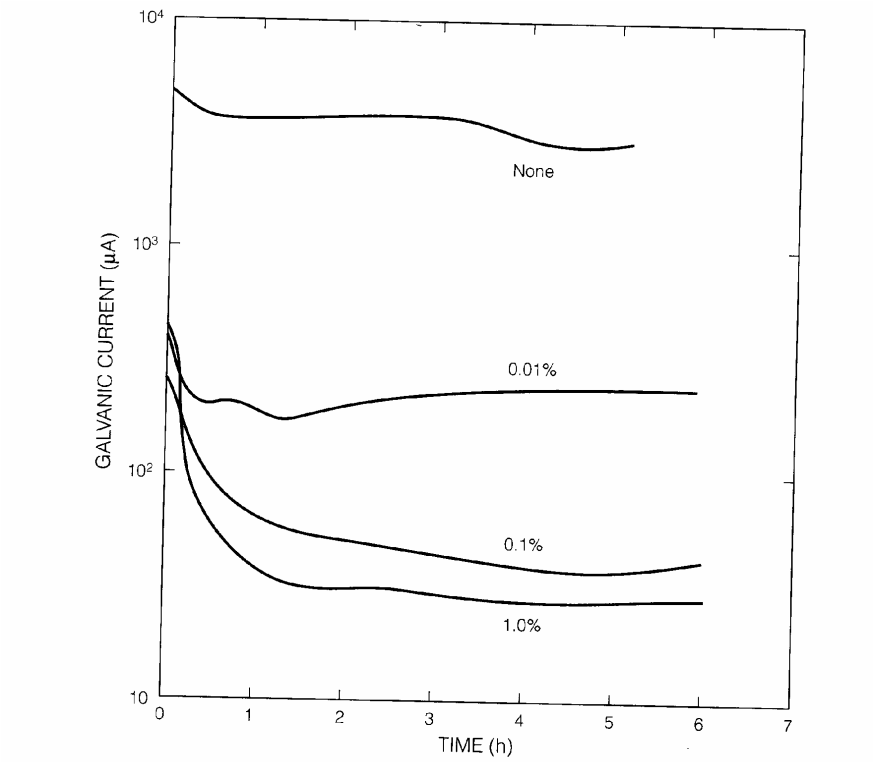

FIGURE 6.15 Galvanic couple currents between brass and steel recorded automatically from a potentiostatic zero resistance ammeter. Effect of added $K_2Cr_2O_7$ in aerated 20% NaCl. *(From D. A. Jones,* Corrosion, *Vol. 40, p. 181 1984. Reprinted by permission, National Association of Corrosion Engineers.)*

Determining Rates of Galvanic Corrosion:

The rate of galvanic attack in a two metal couple is measured by the galvanic current density at the anode. The anodic current density on any point on the anode depends on the polarization of both, anode and cathode, on the conductivity of the solution and the physical geometry of the couple.

Anodic and cathodic polarization curves are used to visualize the polarization within a galvanic couple. The two curves can be obtained in two separate experiments using a potentiostat. A composite polarization diagram for different metals and alloys in aerated 3% NaCl is shown in figure 6.17. The intersection of an anodic curve with a cathodic curve of a more noble metal gives the couple current and potential. The dashed vertical lines in figure 6.17 represent the spread of values for the limiting current for reduction of dissolved oxygen, which is essentially the same for all alloys listed. A prediction of the surface area ratio (figure 6.17 corresponds to 1 cm^2 surfaces for both electrodes) can again be made by graphically increasing the cathodic current. This is shown in more detail in figure 6.19. The new galvanic current has risen by a factor of 10. But the anodic surface area is still 1 cm^2, the anodic current density is now 700μAcm^{-2}. However, the surface of the cathode has increased leading to a

cathodic current density of only 70μAcm^{-2}.

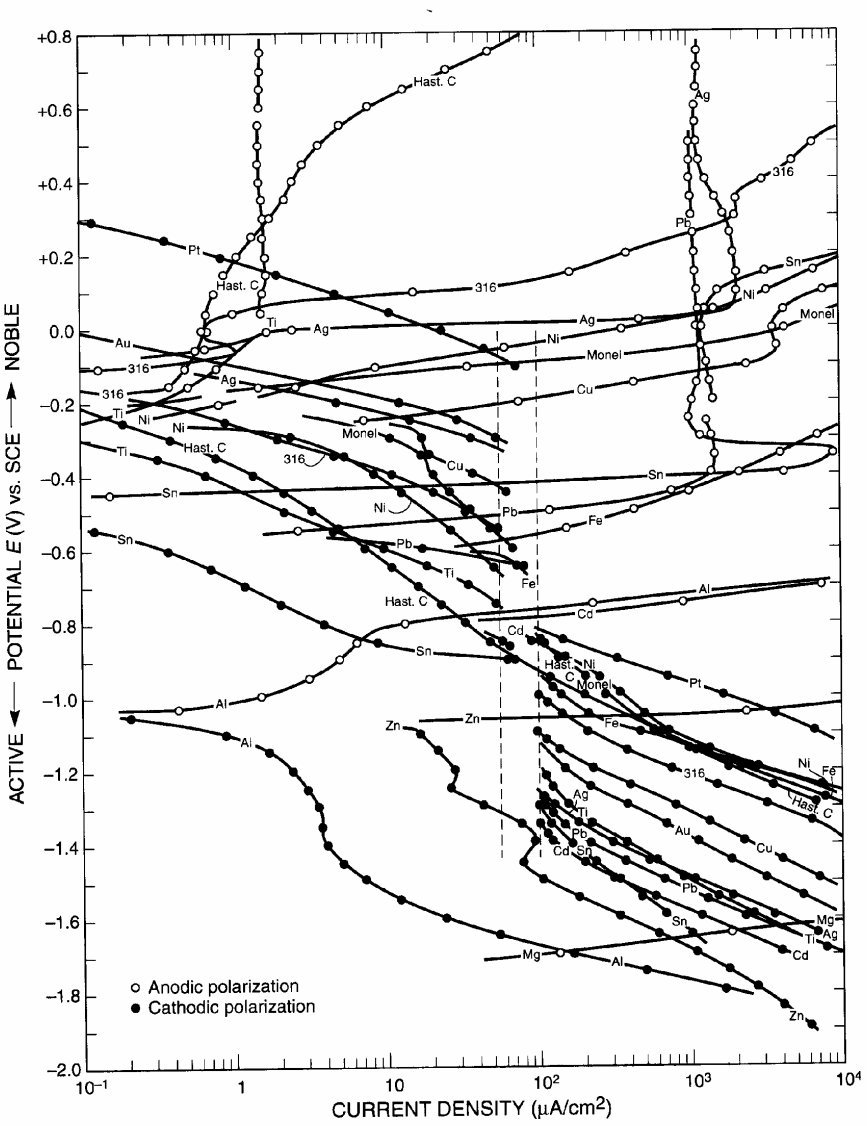

FIGURE 6.17 Potentiostatic polarization curves for various metals and alloys for prediction of galvanic corrosion in aerated 3% NaCl. *(From Bennett and Greene[7].)*

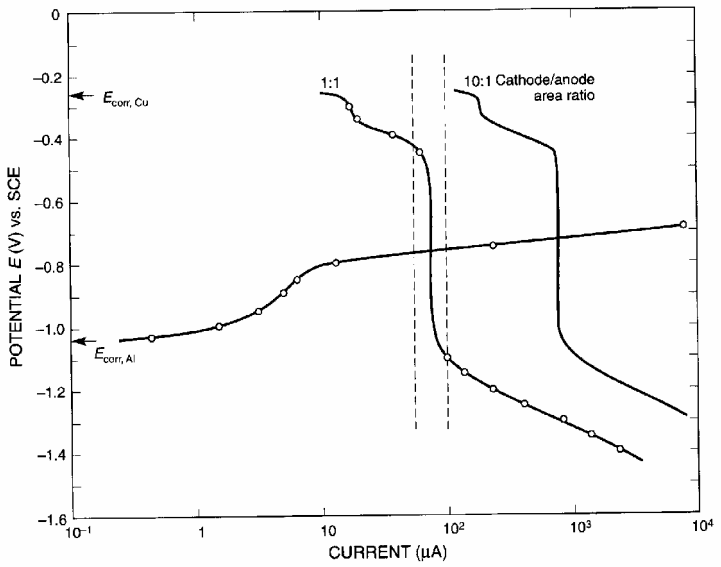

FIGURE 6.19 Predicting galvanic corrosion rates of aluminum-copper couples: Effect of Cu:Al surface area ratio. Polarization curves for Cu and Al taken from Figure 6.17.

Potentiostatic polarization curves again have to be used with caution, for predicting corrosion behavior, as real environments tend to differ from controlled experiments. The influence of the solution can be seen when figure 6.17 for NaCl is compared to figure 6.18 for a deaerated 1N surfuric acid solution.

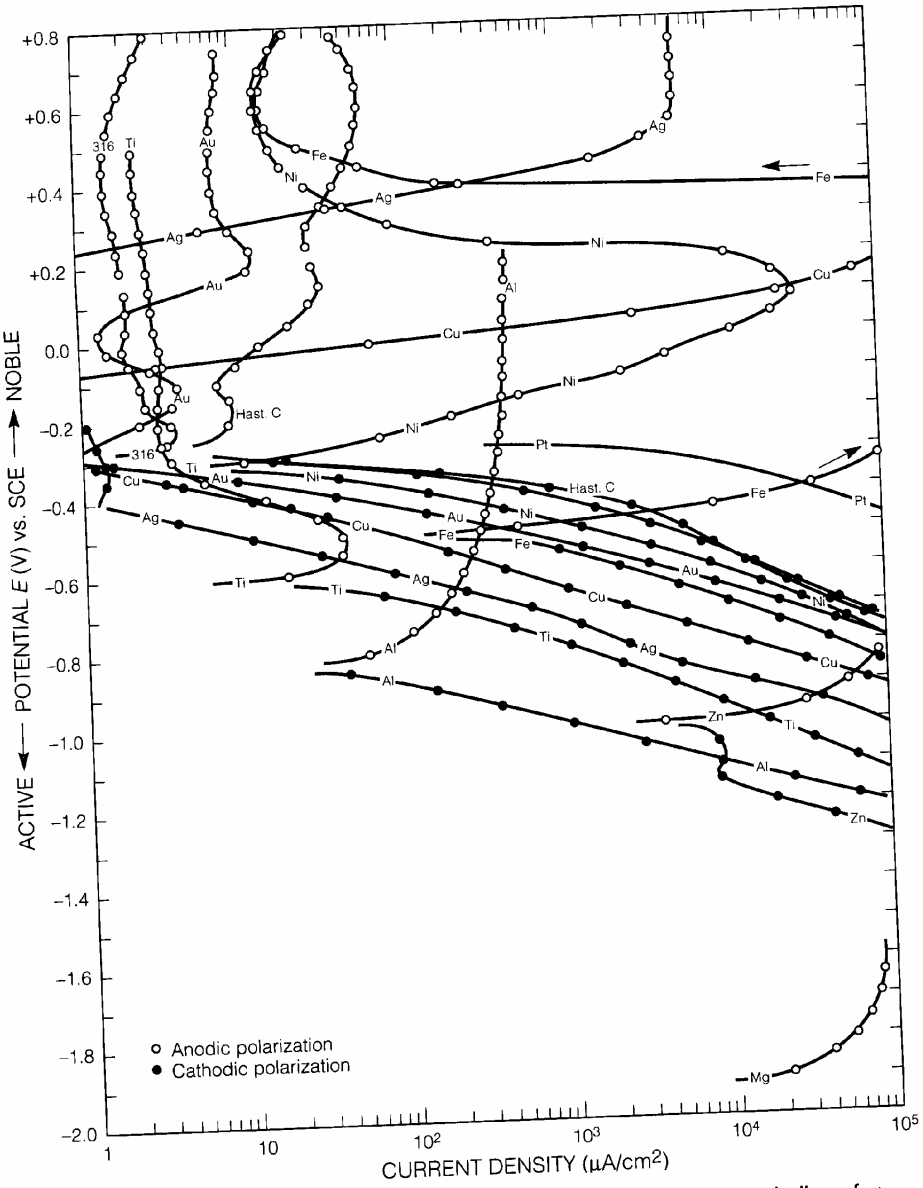

FIGURE 6.18 Potentiostatic polarization curves for various metals and alloys for prediction of galvanic corrosion in deaerated 1*N* H_2SO_4. *(From Bennett and Greene[7])*

Galvanic Passivation of Titanium:

When Ti is coupled to Pt, Pd, Rh or Ir the couple current is dominated by the hydrogen reaction at a potential within the passive range of Ti. This is used to give Ti corrosion resistance to hot acidic solutions can therefore be obtained by alloying these elements to Ti. A

similar effect can be reached using Ni. The polarization curves for Ti and Pt (Ni) are shown in figure 6.20.

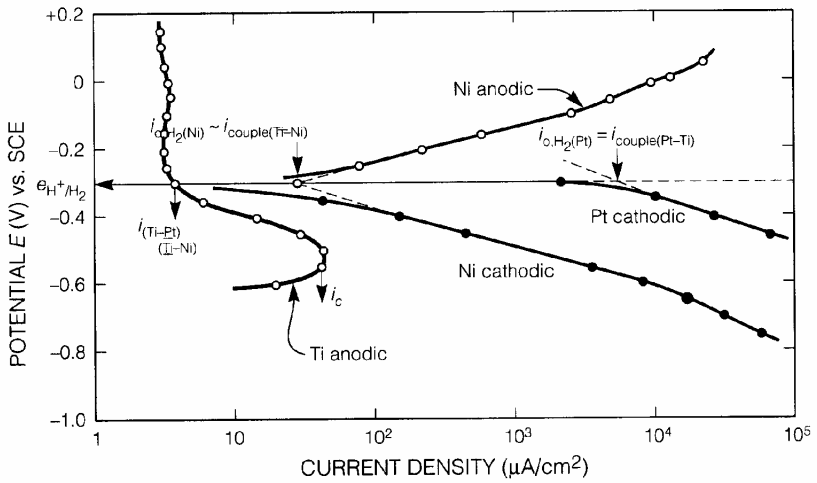

FIGURE 6.20 Polarization curves taken from Figure 6.17 illustrating galvanic passivation of Ti when coupled to Pt or Ni.

Current and Potential Distributions:

Until now uniform current distribution on the surface was assumed. In practice this assumption does not hold. The current and potential distributions between two coupled metals depend on the conductivity of the electrolyte, the physical geometry and on the polarization of anode and cathode. Solution conductivity leads to an ohmic drop R_Ω, between any pair of points on anode an cathode. This leads to a reduced current $I<I_{couple}$. The potential distribution within the solution under a steel and Ni couple is shown by lines of constant potential in figure 6.21.

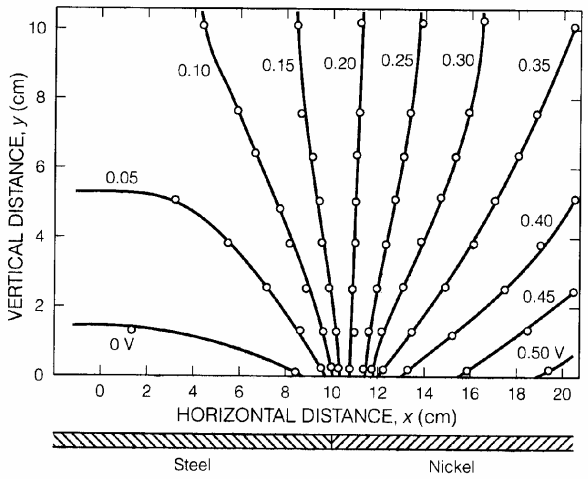

FIGURE 6.21 Potential distribution around a coplanar galvanic couple between iron and nickel. *(From H. R. Copson,* Trans. Electrochem. Soc., *Vol. 84, p. 71, 1943. Reprinted by permission, The Electrochemical Society.)*

The Ni cathode is obviously highly polarized in contrast to the steel anode. This leads to increased corrosion near the contact point on the steel and decreased corrosion near the contact point in the Ni.

Concentration Cells:

Corrosion is often affected by concentration calls. Differential aeration with different concentrations of dissolved oxygen on a single metal surface or on electrically connected surfaces are common. Such cells are especially important for Fe and carbon steels. Acid chloride concentration cells are important for the initiation and growth of pitting and crevice corrosion in stainless steel.

A laboratory setup of a differential aeration cell is shown in figure 6.23. Two iron electrodes are immersed in 0.1 N NaCl on both sides of a porous diaphragm, allowing charge transfer, but not sufficient mass transfer to affect the dissolved oxygen content.

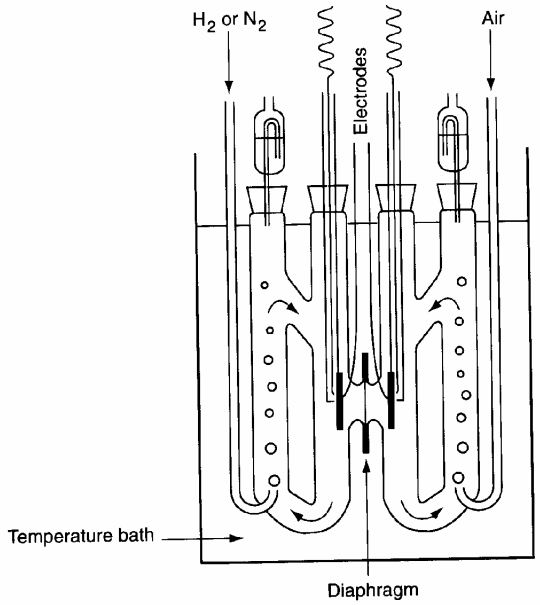

FIGURE 6.23 Differential aeration cell. *(From H. Grubitsch, cited by U. R. Evans, The Corrosion and Oxidation of Metals, Arnold, London, p. 129, 1960.)*

For uncoupled electrodes the anodic and cathodic reactions on the nitrogen side are

$$Fe \rightarrow Fe^{2+} + 2e^-$$

$$2H_2O + 2e^- \rightarrow 2OH^- + H_2.$$

As there is hardly any dissolved oxygen, reduction of dissolved oxygen as the cathodic reaction is impossible. On the aerated side the anodic reaction is still the oxidation of Fe, but the cathodic reaction is the reduction of the dissolved oxygen by

$$O_2 + 2H_2O + 4e^- \rightarrow 4OH^-$$

The Ni cathode is obviously highly polarized in contrast to the steel anode. This leads to increased corrosion near the contact point on the steel and decreased corrosion near the contact point in the Ni.

Concentration Cells:

Corrosion is often affected by concentration calls. Differential aeration with different concentrations of dissolved oxygen on a single metal surface or on electrically connected surfaces are common. Such cells are especially important for Fe and carbon steels. Acid chloride concentration cells are important for the initiation and growth of pitting and crevice corrosion in stainless steel.

A laboratory setup of a differential aeration cell is shown in figure 6.23. Two iron electrodes are immersed in 0.1 N NaCl on both sides of a porous diaphragm, allowing charge transfer, but not sufficient mass transfer to affect the dissolved oxygen content.

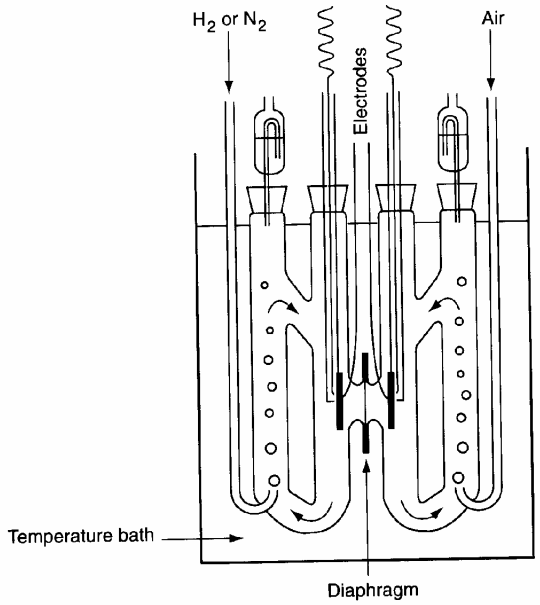

FIGURE 6.23 Differential aeration cell. *(From H. Grubitsch, cited by U. R. Evans, The Corrosion and Oxidation of Metals, Arnold, London, p. 129, 1960.)*

For uncoupled electrodes the anodic and cathodic reactions on the nitrogen side are

$$Fe \rightarrow Fe^{2+} + 2e^-$$

$$2H_2O + 2e^- \rightarrow 2OH^- + H_2.$$

As there is hardly any dissolved oxygen, reduction of dissolved oxygen as the cathodic reaction is impossible. On the aerated side the anodic reaction is still the oxidation of Fe, but the cathodic reaction is the reduction of the dissolved oxygen by

$$O_2 + 2H_2O + 4e^- \rightarrow 4OH^-$$

The corrosion rate of the uncoupled cathode is controlled by concentration polarization and diffusion of dissolved oxygen at $I_{L,C}$. The uncoupled corrosion potential on the aerated electrode is $E_{corr,\,C}$ as shown in figure 6.24.

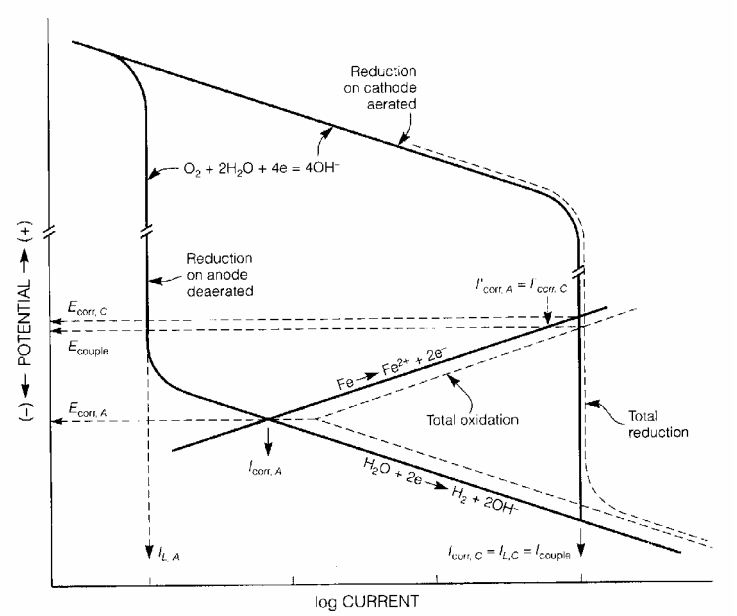

FIGURE 6.24 Mixed potential analysis of the differential aeration on identical iron electrodes of equal area, assuming uniform constant solution concentration and current distribution.

When the two sides are coupled one finds the couple potential between the two initial potentials. The potential distributions on the surface again lead to increased attack near the junction. On the aerated side the reduction reaction leads to an increase in pH, whereas at the deaerated side the Fe^{2+} ions react with water leading to a decrease in pH by the reaction

$$Fe^{2+} + 2H_2O \rightarrow Fe(OH)_2 + 2H^+$$

Increased alkalinity passivates the cathode and increased acidity increases the activity of the anode. This addiditonal effect is shown schematically in figure 6.25.

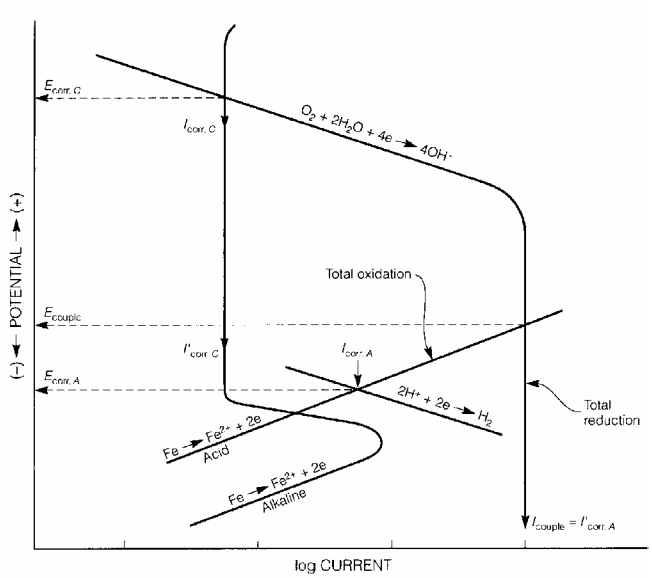

FIGURE 6.25 Mixed potential analysis of a differential aeration cell on iron with passivated cathode and acidified anode.

This effect can be clearly seen at waterline corrosion on steel and zinc. Corrosion depletes the water from dissolved oxygen, which is easiest replaced near the surface of the water in an unstirred solution. Depleted oxygen creates the anode at greater depth and the cathode formed at the waterline by reduction of the excess dissolved oxygen. This is schematically shown in figure 6.26.

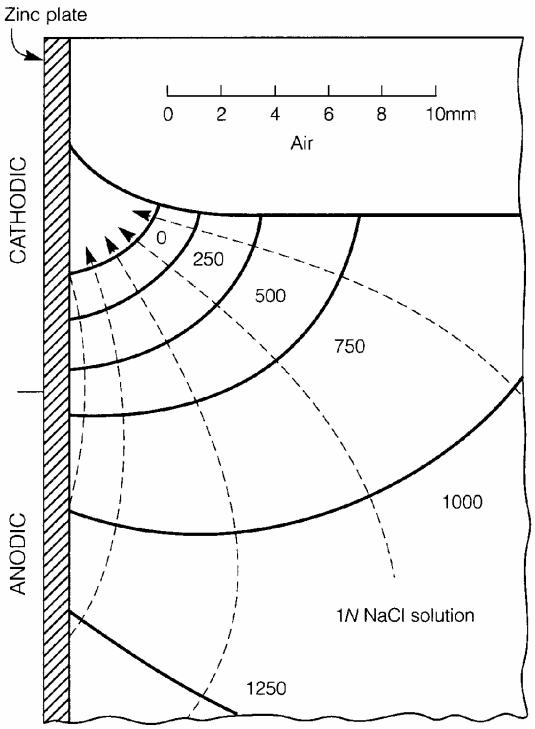

FIGURE 6.26 Potential (solid) and current (dashed) distributions on a vertically immersed zinc plate at the water line. *(From J. N. Agar and U. R. Evans, cited by Kaesche[18].)*

The surface at the waterline is passivated by formation of local alkalinity from reduction of dissolved oxygen. But the metal is strongly attacked nearby, where dissolved oxygen is less accessible, but solution resistance is minimized between adjacent surfaces. This process can be shown by putting a drop of saltwater on an abraded steel surface. In the water small amounts of phenolphthalein and ferricyanide indicators show cathodic areas pink (OH^- formation) and anodic areas blue (liberation of Fe^{2+}). The initial and final surface distributions are shown in figure 6.27. Similar concentration cells can also form when the metal is fully immersed. One has found concentration cell corrosion in both agitated and quiescent solutions. But in full immersed experiments the formation of the concentration cells takes longer times up to several days. So anodic and cathodic areas can form at a surface even if the solution flows, which one would think should lead to a homogeneous aeration of the solution.

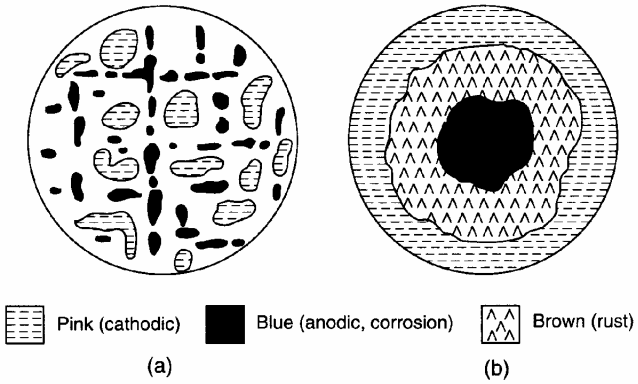

FIGURE 6.27 Initial (a) and final (b) distribution of anode and cathode in a water drop on a horizontal iron surface. *(From U. R. Evans,* An Introduction to Metallic Corrosion, *Arnold, London, p. 36,1981. Reprinted by permission Edward Arnold Publishers Ltd.*